

Review

Molecularly Imprinted Plasmonic-Based Sensors for Environmental Contaminants—Current State and Future Perspectives

Tamara Lazarević-Pašti , Tamara Tasić, Vedran Milanković and Nebojša Potkonjak

Department of Physical Chemistry, VINČA Institute of Nuclear Sciences (National Institute of the Republic of Serbia), University of Belgrade, Mike Petrovica Alasa 12-14, 11000 Belgrade, Serbia

* Correspondence: lazarevictlj@yahoo.com or tamara@vin.bg.ac.rs

Abstract: The increase of production and consumption persistently introduce different pollutants into the environment. The constant development and improvement of analytical methods for tracking environmental contaminants are essential. The demand for high sample throughput analysis has hit the spotlight for developing selective sensors to avoid time-consuming sample preparation techniques. In addition, the sensor's sensitivity should satisfy the rigorous demands of harmful compound tracking. Molecularly imprinted plasmonic-based sensors are excellent candidates to overcome selectivity and sensitivity issues. Molecularly imprinted polymers are robust, stable in aqueous and organic solvents, stable at extreme pHs and temperatures, and include a low-cost synthesis procedure. Combined with plasmonic-based techniques, they are the perspective choice for applications in the field of environmental protection. Plasmonic-based sensors offer a lower limit of detection, a broad linearity range, high sensitivity, and high selectivity compared to other detection techniques. This review outlines the optical plasmonic detection of different environmental contaminants with molecularly imprinted polymers as sensing elements. The main focus is on the environmental pollutants affecting human and animal health, such as pesticides, pharmaceuticals, hormones, microorganisms, polycyclic aromatic hydrocarbons, dyes, and metal particles. Although molecularly imprinted plasmonic-based sensors currently have their application mostly in the biomedical field, we are eager to point them out as a highly prospective solution for many environmental problems.

Keywords: pollutant; environment; pesticides; pharmaceuticals; hormones; microorganisms; polycyclic aromatic hydrocarbons; dyes; metal particles



Citation: Lazarević-Pašti, T.; Tasić, T.; Milanković, V.; Potkonjak, N. Molecularly Imprinted Plasmonic-Based Sensors for Environmental Contaminants—Current State and Future Perspectives. *Chemosensors* **2023**, *11*, 35. <https://doi.org/10.3390/chemosensors11010035>

Academic Editors: Verónica Montes García and Alexander Castro Grijalba

Received: 6 December 2022

Revised: 27 December 2022

Accepted: 29 December 2022

Published: 2 January 2023



Copyright: © 2023 by the authors. Licensee MDPI, Basel, Switzerland. This article is an open access article distributed under the terms and conditions of the Creative Commons Attribution (CC BY) license (<https://creativecommons.org/licenses/by/4.0/>).

1. Introduction

Environmental pollution is one of the main threats to the health of all living beings nowadays. Humans and animals are all affected by different contaminants found in the environment, mostly caused by androgenic factors. There are many ways of pollutant entrance into the natural environment. Some are industrial waste, traffic gas emissions, biomedical waste, and the chemicals used in agricultural production. The most common pollutants are persistent organic and pseudo-persistent pollutants, including different pharmaceuticals, pesticides, dyes, metallic particles, etc. [1–5]. Special attention nowadays is placed on pesticides and pharmaceutical residues in water, since chronic exposure to them can be linked with severe consequences and long-term effects. Moreover, these compounds pose a particular challenge for wastewater treatment, as they cannot be filtered out completely, so they make their way into terrestrial and aquatic environments. Residues of pesticides and pharmaceuticals have been detected in surface water and groundwater worldwide. Of the greatest concern are organophosphorus pesticides, hormones, antibiotics, and analgesic medications. They have the highest environmental potency and risk since they can target the endocrine system (so-called endocrine disruptors, ED) or can

contribute to antimicrobial resistance (AMR). Numerous potential diseases are linked to ED, including reproductive and endocrine (e.g., breast or prostate cancer, infertility, diabetes, early puberty), immune and autoimmune, cardiopulmonary, and nervous systems (e.g., Alzheimer's disease, Parkinson's disease, and attention deficit hyperactivity disorder) [6]. On the other hand, the overuse of antibiotics in human health and agriculture practices causes releases into the environment, which is a vector of AMR. The wastewaters become a reservoir for resistant genes and the development and spread of resistance to pathogens [7]. Therefore, the detection and removal of these pollutants remain burning issues in the modern world to prevent harmful impacts on various ecosystems and human health due to direct exposure to these contaminants.

One health principle is a new global initiative for overcoming these burning problems. It is an approach that recognizes that people's health is closely related to the health of animals and the environment (Figure 1). This concept is not exactly new but has been neglected for many years. One of the main One Health issues is the contamination of the water used for drinking or recreation, especially with respect to pollution management and combating antimicrobial resistance. To make the One Health approach work, it is essential to implement joint responses of Government officials, researchers, and the community to health threats. With this in mind, developing new solutions that address the root causes of One Health issues is a high priority worldwide.

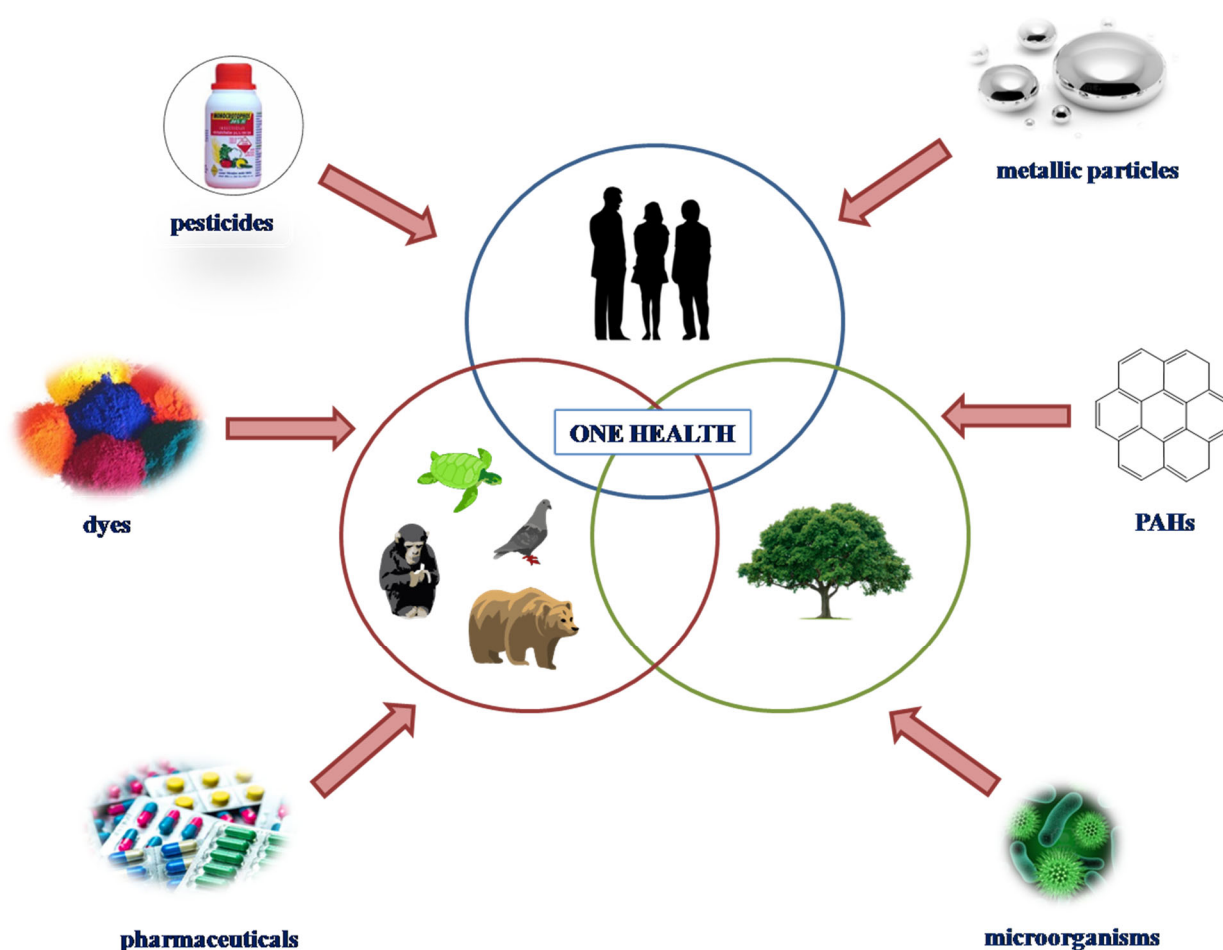


Figure 1. Schematic representation of the One Health principle.

Many efforts were made to develop new methods that allow the detection of potential pollutants with the goal of their real-time and in situ monitoring [5,8,9]. Chemical sensors are an attractive technology to achieve this goal. They are portable, robust, have a quick response, and usually have low-cost manufacturing and operation. Moreover, there is a

wide variety of chemical sensors (e.g., optical sensors, electrochemical sensors, electromechanical sensors, etc.) [5,10–14], which can be chosen based on the type of environmental contaminant. Nevertheless, chemical sensors sometimes have poor selectivity, which makes the monitoring of target pollutants in complex samples, such as environmental, a difficult task. Molecularly imprinted polymers (MIPs) as recognition elements are a great choice to overcome this problem. In combination with optical plasmonic sensing methods, it is possible to construct devices with satisfactory properties in terms of selectivity, sensitivity, and stability.

This contribution provides an overview of the optical plasmonic detection of different environmental contaminants with MIPs as sensing elements, as well as their comparison with the other types of sensors developed for respective pollutant detection. In addition, we will provide a brief background of molecularly imprinted plasmonic sensor development and a synopsis of the most relevant environmental contaminants. The spotlight of this paper is on the environmental pollutants that affect the health of humans and animals. Pesticides, pharmaceuticals, hormones, microorganisms, polycyclic aromatic hydrocarbons (PAHs), dyes, and metal particles stand out within this wide group. The review covers recent advances in stable, reproducible, and cost-effective plasmonic sensors for mentioned environmental contaminant detection. The work focuses on their most important properties, such as the limit of detection (LOD), linearity range (LR), selectivity, sensitivity, stability, and reusability. Additionally, we will thoroughly compare the performances of these specific and innovative sensors with different sensing methods for the particular pollutant detections available in the literature. To the best of our knowledge, no review article currently covers this specific topic.

2. Background of Molecularly Imprinted Plasmonic Sensors

A sensor is a device that detects input from the physical environment and responds to it. The response is usually a signal that is converted to a human-readable display. The sensor consists of a receptor and transducer. The receptor is responsible for transforming the information contained in the analyte into energy that the transducer can measure, and it ensures the selectivity of the sensor. A transducer is a device capable of transforming the energy contained in the analyte into an analytical signal. Sensors can be classified in many ways, but, most often, the classification is based on the working principle of the transducer or the nature or recognizing element within the receptor. Based on the type of transducer, the most commonly used are electrochemical and optical sensors. Among possible sensor receptors, bio and biomimetic sensor elements are the most selective ones.

The selectivity of a sensor is the most challenging aspect of its construction. It is defined as the ability of a sensor to distinguish the target from the interfering molecules and display a target-specific response. In biosensors, the receptor can be made of various biomaterials: enzymes, antigens/antibodies, DNA probes, tissue, cells, and cell organelles. These recognition elements provide excellent sensitivity, repeatability, and sensor accuracy. The ability of a large number of samples to be analyzed, rapid and continuous detection to be provided, low chemical reagent usage, reuse of biological elements, online measurements, constant recording, and an ultra-sensitive nature of biosensors are their main advantages. On the other hand, sensors with biological origin receptors are expensive and hard to handle, since many factors influence their stability. They can easily lose activity due to deactivation after a relatively short period. Biosensors have longer recovery times. In addition, their stability depends on pH, temperature or ion concentration, and narrow or limited temperature range.

In biomimetic receptors (receptors without a biological origin), synthetic molecules have in their structure functional groups able to selectively interact with the analyte. They are cheaper and more stable than bioreceptors, making them desirable for use. Biomimetic receptors can be made of non-protein catalysts, calixarenes, molecularly imprinted polymers, aptamers, and nanomaterials. The host–guest principle is crucial for their role as a receptor.

Molecularly imprinted polymers are an attractive option to overcome the selectivity problem. MIPs are synthetic materials with recognition abilities towards specific species through imprinted binding sites on the polymeric matrix [5,15–17]. They are robust, plastic-based materials, cheap to synthesize, and prone to be reused. The molecular imprinting process implies functional monomer polymerization in the presence of the target analyte, called a template (Figure 2). After the formation of the polymer, the template is removed. The template leaves a 3D cavity (binding site) in the polymeric structure behind, with the size and shape of the template and functional groups with specific orientations ready to interact with the target analyte [5,18]. The advantages of MIPs compared to other receptor molecules are their selectivity, robustness, stability in aqueous and organic solvents, stability at extreme pHs, reported working temperatures to range from 0 to 150 °C (suitable for sterilization), and low-cost synthesis procedure. In addition, the plethora of monomers with different functional groups available for their synthesis enables them to offer a great variety of formats, sizes, shapes, and supports in which MIPs can be easily prepared. Those characteristics are particularly important, as they make them ideal candidates to be easily combined with sensing devices to enhance their selectivity considerably. MIPs can be obtained in many formats, from macro- to micro- and nanosized, thick to thin sub-nanometer-layers, and micro- to nanoparticles. In addition, they can be easily integrated into devices and electronics. The resourcefulness of MIPs appears perfect for achieving the desired selectivity and simultaneously opens up the possibility of exploring new sensor configurations [19].

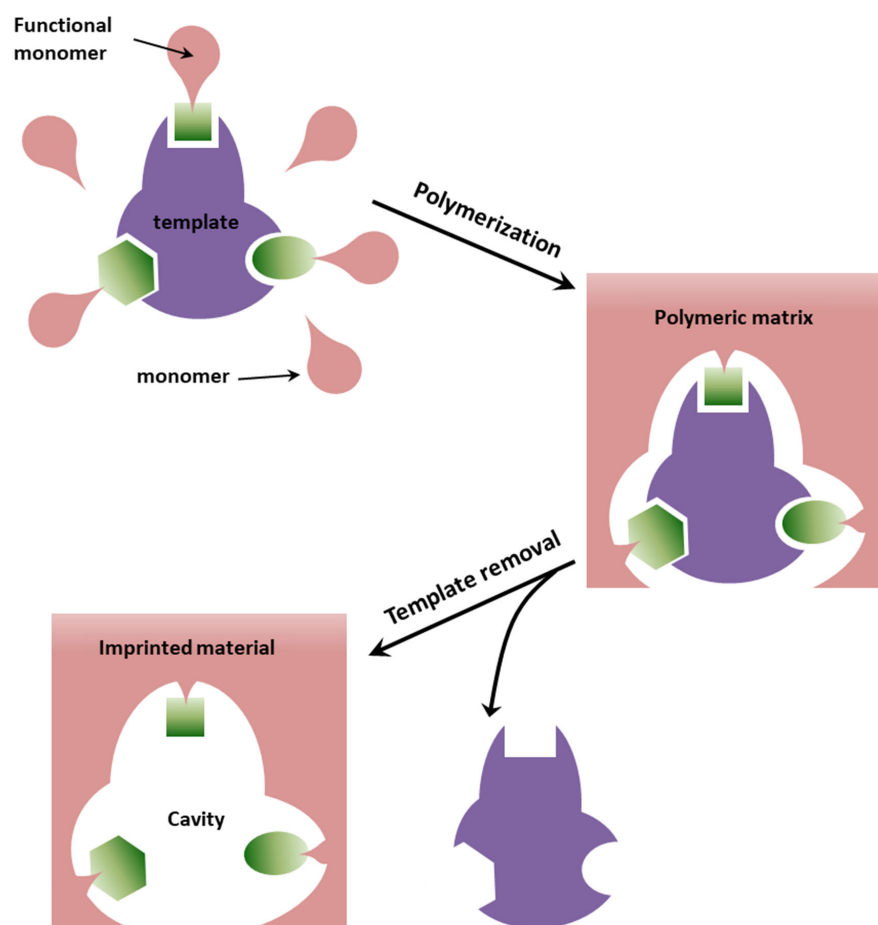


Figure 2. The molecular imprinting process.

Nowadays, MIPs have been integrated into many sensing platforms and assay formats for the detection of various targets. They were shown to be a good choice for different target analytes, including small molecules, as well as macromolecules and whole cells [20].

The basis of optical sensor development includes various technologies of optical phenomena, which are the result of the correlation of an analyte with the receptor part [21,22]. They can be further subdivided according to the type of optical properties, such as reflectance, absorbance, refractive index, fluorescence, luminescence, and light scattering [22,23]. Optical sensors are characterized by fast responses and direct label-free detection. They also exert the ability to monitor target analytes in complex environments. Highly significant optical sensors endure the criteria of robustness, miniaturization, and the possibility to operate in remote mode [19,24,25]. Furthermore, when optical sensors are based on plasmonic phenomena [22,26], they provide the ability for extreme light control. It enables additional analytical advantages, such as determinations down to the single molecule, *in vivo* and *in situ* [22,27].

Plasmonics-based optical sensors have been under development for over 40 years. They are attractive because of their advantages compared to conventional sensors. First of all, plasmonic-based sensors are capable of real-time monitoring. Secondly, they enable label-free detection and provide high reusability, short response time, and simple sample treatments. Moreover, plasmonic-based sensors use minimal electrical components. On the other hand, plasmonic sensors have some disadvantages, too. They are nonspecific toward the binding surface, limited by mass transportation, susceptible to steric hindrance during the binding event, and carry a risk of data misinterpretation during common events [28,29]. Plasmonic-based methods include surface plasmon resonance (SPR), localized surface plasmon resonance (LSPR), surface-enhanced Raman scattering (SERS), surface-enhanced fluorescence (SEF), and surface-enhanced infrared absorption spectroscopy (SEIRA) [29].

Surface plasmon resonance refers to the electromagnetic resonance of the collective oscillations of the free electrons from the plasmonic metal-dielectric interface. Due to the resonance, the coupled propagating electromagnetic field (EM) is created along the metal-dielectric interface. This field exponentially decays in both media and is highly sensitive to the refractive index change of the dielectric layer [30]. Conventional SPR-based sensors consist of the high-index prism, plasmonic metal (gold or silver for visible spectrum), and dielectric/sensing layer. The total internal reflection of the electromagnetic wave takes place on the prism-metal interface. In the case of resonance, a large fraction of light is passed on the metal-dielectric interface as a surface wave, which leads to a sharp dip in the reflection spectrum [31]. Besides prism-based, nowadays optical-, grating-, and chip-based SPR sensors are in use. Chip-based SPR sensors allow label-free detection and dynamic measurement of binding-unbinding kinetics and are highly sensitive [29].

Localized surface plasmon resonance-based sensors represent a type of SPR-based sensor where the resonant EM field is limited to the metallic nanostructure and a medium (sensitive to reflective index change) surrounding it within a few tens of nm. Besides the medium, the shape, size, and material of the plasmonic nanostructures impact the resonance conditions. Nanoparticle dimensions are crucial to determine resonance wavelength, scattering to absorption ratio, and extinction cross-section. The general development of this type of sensor includes fabricating metallic nanostructures with an overlayer of the sensing film [32]. Thanks to the development of nanolithography, LSPR-based sensors use colloidal particles and chip-based substrates with high sensitivity and repeatability [29].

Surface-enhanced fluorescence-based sensors are established on the increase of the fluorescence intensity of a fluorophore material using plasmonic nanomaterial. This effect manifests by bringing the fluorophore close to the metallic nanostructure enough that the local plasmonic electric field is coupled with the fluorophore electrons. It leads to an increased electric field that fluorophore experiences and, therefore, an enhanced fluorescence emission [33]. The selection of the fluorophore and metal is limited to those combinations in which optical absorption bands overlap [29].

Surface-enhanced Raman scattering-based sensors have become a dominant analytical tool in many fields in the past few years. SERS technology enabled the enhancement of the naturally weak Raman signal via the optical and chemical properties of accessible plasmonic nanomaterial. The main advantage of this type of sensing is the high selectivity

enabled by the unique fingerprint of the analyte. In addition, the sample preparation method is easy, and there is no signal interference from the medium. Moreover, it is possible to perform a single-molecule detection. The plasmonic metallic nanostructures have a localized EM field due to LSPR. Therefore, they would enhance the Raman signal of the Raman-active material if the material is near the plasmonic nanostructure [34]. The enhancement of the Raman signal is up to 10^{10} times. It occurs as a result of two types of processes: EM or chemical processes. EM enhancement contributes dominantly, up to 10^8 times, and chemical enhancement increases the signal up to 100 times. SERS has many advantages, including high selectivity, easy sample preparation, no signal interference from the analyte medium, and single molecule detection [29].

Surface-enhanced infrared absorption-based sensors are based on the enhancement of the IR absorption signal of a target material in the presence of a plasmonic nanostructure. Because of the wavelength range of IR spectroscopy, SEIRA-based sensors can use other plasmonic nanomaterials besides gold and silver, such as other metals, semiconductors, and graphene. To achieve resonance in the IR range, a nanoantenna-type structure has to be designed so that its length is equal to multiple numbers of half the effective wavelength, making this technique expensive and hard to do [29,35].

The basic principles of plasmonic-based detection methods are presented in Figure 3.

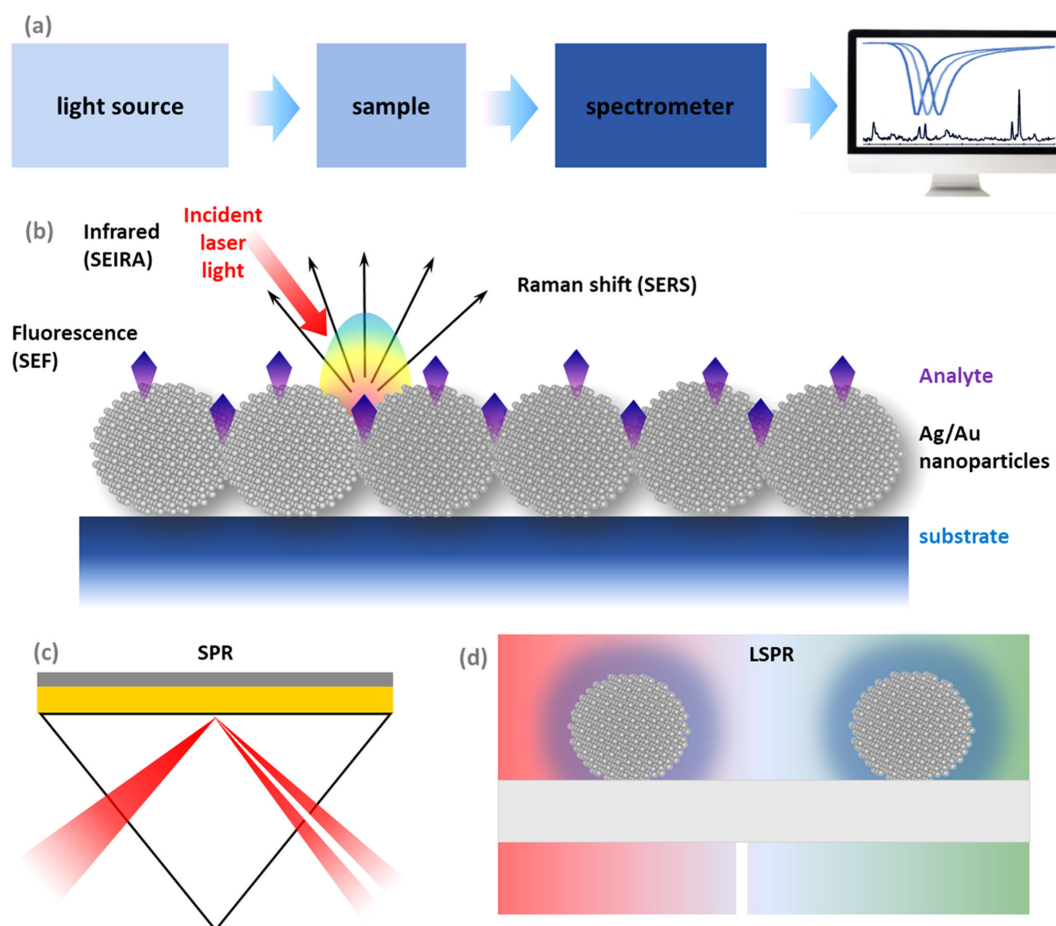


Figure 3. The basic principles of plasmonic-based detection methods. (a) General scheme of a plasmonic-based sensor; (b) SERS, SEF, and SEIRA; (c) SPR; (d) LSPR.

Key points in building an imprint sensor with plasmonic detection are an adequate choice of polymer, selection of technique in the process of synthesis of MIP, and means of the detection. The techniques for MIP synthesis can be in situ and ex situ. In situ synthesis implies that the imprinted polymer is prepared on the transducer, and the ex situ technique

means that the imprinted polymer is prepared separately from the transducer. A UV-VIS spectrophotometer, spectrofluorimeter, Raman, and FTIR spectrometer can be used for the detection of an analyte in MIP plasmonic sensors.

One of the biggest problems hindering the development of MIP plasmonic sensors is also one of their most significant advantages—their selectivity. As the MIP plasmonic sensors are highly selective towards only one specific compound, it disables them from being used in multi-analyte sensor construction. Therefore, it makes them undesirable for industrial applications. The adequate choice of materials and detection methods affects sensitivity and reproducibility the most. It is also necessary to take the cost of sensor components into account.

The leading methods for solving these problems are the further development of low-cost MIP plasmonic sensor components by introducing novel materials and using a set of different MIPs to detect multiple analytes at once. In addition, combining plasmonic detection with electrochemical methods could significantly improve the sensitivity and reproducibility of this type of sensor.

3. Major Environmental Contaminants and Molecularly Imprinted Plasmonic-Based Sensors for Their Detection

3.1. Pesticides

Pesticides are substances or mixtures of substances whose purpose is to prevent, destroy, or control any pests, such as insects, fungi, rodents, or weeds. They can be classified according to their origin into chemical pesticides and biopesticides. With respect to the mode of action, pesticides are systemic or non-systemic, and, according to the targeted types of pests, are listed as insecticides, fungicides, herbicides, and rodenticides. Most often, pesticides are referred to according to their chemical composition as organochlorines, organophosphorus, carbamates, pyrethroids, amides, anilines, and nitrogenous heterocyclic compounds. Organochlorine, organophosphate, and carbamate pesticides are highly toxic, and later-developed pyrethroids, amides, anilines, and nitrogenous heterocyclic compounds are considered less harmful.

Pesticides are widely used in agricultural, commercial, and residential settings, making exposure to the general population ubiquitous. Before, pesticides were considered acutely toxic and not carcinogenic. In the past decade, an increasing number of case-controls, cohort studies, and meta-analyses with exposure information on pesticides and other etiologically relevant factors have investigated hypotheses linking occupational and environmental pesticide exposure to several different cancers. Moreover, evidence is emerging that chronic low-dose exposure to various pesticides perturbs many biologic pathways, including oxidative stress [36] and immunotoxicity [36], that have been linked with carcinogenesis. There is evidence that pesticides could be responsible for developing prostate, lung, colorectal, and pancreatic cancer, and melanoma, multiple myeloma, and leukemia [36].

Considering the increased world population and, therefore, the need for increased food supplies, increased use of pesticides is expected. However, with the increasing and frequent use of pesticides, in addition to many advantages, corresponding negative effects can be observed. Many pesticides, as artificial organic compounds, are not biodegradable and, due to bioaccumulation, can enter the food chain and affect the entire environment. Toxic effects on human health and ecosystems include acute and persistent damage to the nervous system, lung damage, reproductive organ damage and dysfunction of the immune and endocrine systems, congenital disabilities, and cancer. Based on this, it is very important to control, monitor, and remove pesticides from the environment.

Among others, organophosphorus pesticides (OPs), widely used in agriculture, are very dangerous and harmful because of their toxic nature. Their toxic effects are primarily attributed to the enzyme acetylcholinesterase's irreversible inhibition (AChE). They also inhibit the other enzymes playing an important role in biochemical processes, such as myeloperoxidase (MPO) [37]. Besides the well-known cholinergic function of AChE, there are indications of AChE involvement in oxidative stress, inflammation, apoptosis, and

cancer development [38]. Acetylcholine level is critical for successfully controlling inflammation and immune response in peripheral tissues [38]. An increase in acetylcholine levels above a certain threshold can suppress pro-inflammatory cytokines' production [38]. Since AChE is responsible for acetylcholine level regulation, its role in modulating inflammation is prominent [38–40]. Furthermore, inflammation is linked to various conditions [38], including cancer, as already mentioned, so this is one more clue suggesting that AChE is involved in these conditions. It is logical to assume that organophosphates, such as AChE inhibitors, are also essential to consider in cancer development.

The view on OPs' effect on the human organism is changing. Once considered only acutely toxic through their influence on AChE, today they are in focus because of increasing evidence of their carcinogenicity. Moreover, their ability to cause anxiety and depression is newly observed and needs to be thoroughly investigated. Epidemiological studies have reported higher incidences of depression in particular groups of individuals, such as those with chronic health conditions [41,42], and individuals in specific occupations, such as farming, fishing, and forestry [42,43]. The reason behind the elevated risk of mood disorders in farming populations is unclear. Some researchers have reported a link between pesticide exposure, mood disorders, and suicidal behavior [42,44]. Organophosphate pesticides, in particular, are associated with an elevated risk of a neuropsychiatric disorder [42,44]. They are the most widely used group of pesticides in the world and are considered by the World Health Organization [42,45] to be one of the most hazardous pesticides to vertebrate animals, responsible for many cases of poisoning worldwide, particularly in developing countries where protective measures are lacking [42,44]. The neurotoxic effects of high-level acute poisoning are well established and involve changes in peripheral, autonomic, and central nervous system function (the cholinergic crisis), resulting in a constellation of physical, cognitive, and psychiatric symptoms. However, OPs disrupt many other neurotransmitters, and some of these are involved in mood regulation, such as serotonin [42,44]. It could explain the link between pesticide exposure and mood disorders observed in earlier studies. This association appears strongest in individuals who report previous instances of acute poisoning [42,44]. However, the impact of long-term low-level exposure to OPs (in doses that do not cause acute toxicity) on human health is less clear. Some studies have found evidence of ill health, mood disorders, and cognitive impairment following low-level exposure to OPs, while others have not [42,44].

The overview and the most important characteristics of MIP-based plasmonic sensors for different pesticide detection are given in Table 1.

As can be seen from Table 1, most MIP-based plasmonic sensors available in the literature today are made for organophosphate pesticide detection, predominantly for chlorpyrifos (CHP) and atrazine (ATZ). Functional monomers usually used for MIP synthesis are MATrp and MAA. Methods used for the detection are SPR and SERS in most cases. All sensors presented in Table 1 are highly selective, with a wide LR and low LOD. Many of them need a few minutes for the analysis, but some require longer periods for detection (up to 20 min).

Besides MIP-based plasmonic sensors for pesticide detection, many other types of sensors were developed to monitor pesticides in the environment. Some of them use MIP as a recognition element but do not have a plasmonic transducer. On the other hand, there are also plasmonic sensors that do not employ MIPs. Many sensors for pesticide detection do not contain an MIP or plasmonic transducer. We aim to compare the characteristic of these sensors with the sensors presented in Table 1.

Table 1. MIP-based plasmonic sensors for different pesticide detection and their most important characteristics.

Analyte	Functional Monomer	Sensor Type	Linearity Range [mol dm ⁻³]	Limit of Detection [mol dm ⁻³]	Response Time [min]	Reference
2,4-dichlorophenoxyacetic acid	MATrp	SPR	(2.3–80) × 10 ⁻¹⁰	1.1 × 10 ⁻¹¹	5	[46]
Amitrole	MATrp	SPR	(6–1190) × 10 ⁻¹¹	3.7 × 10 ⁻¹¹	5	[47]
Ametryn	MAA	SPR	(1–100) × 10 ⁻⁷	3.51 × 10 ⁻⁸	-	[48]
Acephate	MAA	SPR	(5–80) × 10 ⁻¹³	1.14 × 10 ⁻¹³	-	[49]
Atrazine	HEMA	SPR	1 × 10 ⁻¹² –1 × 10 ⁻⁷	1.92 × 10 ⁻¹¹	-	[50]
Atrazine	MAA	Colorimetric/SERS dual chemosensor	-	5.56 × 10 ⁻⁹	15	[51]
Atrazine				9.1 × 10 ⁻¹¹	5	
Simazine	MAPA	SPR	(1–66.4) × 10 ⁻¹⁰	3.1 × 10 ⁻¹¹	3	[52]
Cyanazine				9.5 × 10 ⁻¹¹	3	
Chlorpyrifos	MATrp	SPR	(1.5–290) × 10 ⁻¹¹	-	5	[53]
Chlorpyrifos	Dopamine	SPR	(1–1000) × 10 ⁻⁹	7.6 × 10 ⁻¹⁰	2.5	[54]
Chlorpyrifos	MAA	SERS/colorimetric dual sensor	(2.85–285) × 10 ⁻¹¹	-	<25	[55]
Carbendazim	MAM	SERS	1 × 10 ⁻⁷ –1 × 10 ⁻³	-	-	[56]
Carbofuran			(5–450) × 10 ⁻¹¹	3.5 × 10 ⁻¹¹	5	
Dimethoate	MATrp	SPR	(4–436) × 10 ⁻¹¹	3.3 × 10 ⁻¹¹	5	[57]
Parathion methyl	MAA	SPR	1 × 10 ⁻¹³ –1 × 10 ⁻⁸	-	Fast response	[58]
Paclobutrazol	AM	SERS	(2.55–434) × 10 ⁻⁷	2.55 × 10 ⁻⁷	-	[59]

MATrp—N-methacryloyl-L-tryptophan methyl ester; MAPA—N-methacryloyl-l-phenylalanine methyl ester; HEMA—2-hydroxyethyl methacrylate; MAA—methacrylic acid; MAM—methyl acrylamide; AM—acrylamide.

Xu et al. investigated the detection of CHP using an electrochemical sensor. The sensor is based on an electrode modified with molecularly imprinted polymers, where MAA is used as a functional monomer. The constructed sensor showed high reproducibility, stability, and selectivity towards CHP, with an LR from 1×10^{-10} – 1×10^{-5} mol dm⁻³ and an LOD of 4.08×10^{-9} mol dm⁻³. In addition, the sensor was applied to determine CHP in real samples where recovery varied from 93 to 108% [60]. Comparing these characteristics with the characteristics shown in Table 1 for CHP detection, we can see that MIP plasmonic sensors generally offer better features. The recovery percentage is similar, while the LR is approximately the same, and the LOD is lower.

Fan et al. constructed a molecularly imprinted fluorescent sensor with a structure that uses Mn:ZnS quantum dots as phosphorescent emitters for CHP detection. The sensor showed high selectivity, a fast CHP response (less than 5 min), and an LR of 0 to 8×10^{-5} mol dm⁻³. In addition, the sensor's LOD was shown to be 8.9×10^{-7} mol dm⁻³, and recovery was at 92 to 105% [61]. In contrast to this sensor, MIP plasmonic sensors showed a faster response to CHP (about 2.5 min), a similar recovery percentage in different real samples, and an LR and an LOD three orders of magnitude lower.

Chenggen et al. reported a surface molecular imprinting strategy for synthesizing CHP-imprinted core-shell particles. In combination with a highly sensitive chemiluminescent assay, the method was applied to detect CHP with an LOD of 9.2×10^{-10} mol dm⁻³ and an LR of $(2.5–250) \times 10^{-9}$ mol dm⁻³. The method can also determine CHP in spinach samples with a recovery of 93–106% [62]. By comparing the characteristics of this sensor with sensors presented in Table 1, we can see that they have a range of linearity and an LOD of the same order of magnitude, as well as approximately the same percent recovery in real samples.

Among the non-imprinted plasmonic sensors, a terahertz plasmonic metasurface sensor based on carbon nanotubes, studied by Wang et al., showed a minimum detection mass of 2.85×10^{-11} mol, a sensitivity of 5.7×10^{-9} mol dm⁻³, a good linear relationship between transmission amplitude and CHP concentration, as well as acceptable reliability and stability [63] for the detection of CHP. In addition, Li et al. constructed a direct SPR biosensor based on an oriented assembly of antibodies for rapid detection of CHP. The

biosensor showed good specificity and a low LOD of $1.6 \times 10^{-9} \text{ mol dm}^{-3}$, with an LR of $(7.13\text{--}1426) \times 10^{-10} \text{ mol dm}^{-3}$, where the analysis samples can be performed in just 10 min [64]. Xu et al. have synthesized gold nanoparticles that served as a SERS-active substrate for CHP detection. The SERS method based on gold nanoparticles showed an LOD of $1 \times 10^{-6} \text{ mol dm}^{-3}$, where the sensor was also applied to determine CPH in real samples where the recovery varied from 84.50 to 95.83% [65]. Thepudom et al., in their work, detected CHP using a photoelectrochemical sensor system with surface plasmon resonance. Detection of CHP was achieved at concentrations as low as $7.5 \times 10^{-9} \text{ mol dm}^{-3}$ [66]. In addition, Soongson et al. developed a colorimetric aptasensor for CHP detection that uses SPR of gold nanoparticle aggregates in conjunction with a specific aptamer and cationic polyethyleneimine. Under optimal conditions, the colorimetric aptasensor provides an LR of $(5.7\text{--}85.6) \times 10^{-8} \text{ mol dm}^{-3}$ with a low LOD of $2.1 \times 10^{-8} \text{ mol dm}^{-3}$ where the sensor was applied for analysis in real samples of water, pomelo, and longan (recovery of 85.2–106.3%) [67]. Comparing the aforementioned non-imprinted plasmonic sensors for CHP detection with the MIP plasmonic sensors shown in Table 1 indicates that MIP sensors generally have a wider LR with a lower LOD, a similar percent recovery in real samples, and, usually, faster sensor response.

Zhang et al. have reported the preparation of a gold nanoparticle-thioglycolic acid (TGA@AuNP) suspension for the colorimetric detection of CHP. The synthesized TGA@AuNP colorimetric sensor possesses an LOD of only $5.7 \times 10^{-8} \text{ mol dm}^{-3}$, and a selective sensing response, while the detection time is less than 2 min. [68]. Based on the data shown in Table 1, it is observed that the MIP plasmon sensors have an LOD lower by two orders of magnitude and the detection time is significantly less compared to the colorimetric sensor.

Guler et al. have developed a facile electrochemical biosensor with AChE based on Nafion (NA) and Ag nanoparticles supported on amino-functionalized reduced graphene oxide (rGO-NH₂). The biosensor detected CHP in an LR of $(6\text{--}35) \times 10^{-8} \text{ mol dm}^{-3}$ with an LOD of $4 \times 10^{-8} \text{ mol dm}^{-3}$. In addition, the biosensor NA/Ag@rGO-NH₂/AChE/GCE showed high sensitivity, stability, and reproducibility [69]. Compared to the MIP sensor characteristics in Table 1, this sensor has a three-order-of-magnitude lower LR and a two-order-of-magnitude higher LOD. In contrast, both types of sensors show high sensitivity, stability, and reproducibility.

In addition, Liu et al. reported the development of a magnetically-controlled colorimetric aptasensor for CHP. Under optimal conditions, this Cu-MOF-based magnetically-controlled aptasensor showed an LOD of $1.25 \times 10^{-8} \text{ mol dm}^{-3}$ with an LR of $(0\text{--}3.56) \times 10^{-6} \text{ mol dm}^{-3}$ and a high selectivity for CHP. The aptasensor was also successfully applied for analysis in real samples where the recovery varied in the range of 78–102% [70]. As in the previous case, the aptasensor showed a wider LR with an LOD higher by two orders of magnitude and an approximately similar recovery percentage in real samples compared to MIP plasmonic sensors.

In addition, a nickel composite with oxidized g-C₃N₄ (Oki-g-C₃N₄) was successfully synthesized by hydrothermal treatment by Saranya et al. The Ni/Oki-g-C₃N₄ electrode has an LR of $(1\text{--}15) \times 10^{-15} \text{ mol dm}^{-3}$ with an LOD of $3 \times 10^{-16} \text{ mol dm}^{-3}$ for CHP detection. The sensor showed good sensitivity, stability, and reproducibility, as well as good recovery in the range of 99–99.75% for water samples from wells, lakes, taps, and the sea [71]. Compared to MIP plasmonic sensors, the sensor produced in this way has a lower LR and LOD of six orders of magnitude lower, indicating an exceptional sensitivity for CHP detection. In contrast, the recovery percentage in real samples is very similar.

When we talk about the detection of ATZ using molecularly imprinted sensors without a plasmonic transducer, we can see that Salahshoor et al. developed a sensor by combining a colloidal crystal with the molecular imprinting technique for cheap and simple detection of ATZ in aqueous solutions. The sensor is formed from a 3D interconnected macroporous structure with numerous nanocavities derived from ATZ imprinted in a thin polymer film. The sensor had a dynamic range of $(4.7\text{--}463.5) \times 10^{-10} \text{ mol dm}^{-3}$ for the quantification

of target analyte in aqueous solutions with an LOD of $4.64 \times 10^{-10} \text{ mol dm}^{-3}$ [72]. In addition, Chen et al. have assembled a novel self-powered molecularly imprinted sensor (SPS) based on photo-fuel-driven visible light cells (PFC) with a Ti-Fe-O nanotube, (NTs)/Ni(OH)₂ photoanode, and a functionalized molecularly imprinted polymer cathode. The proposed SPS sensor shows excellent energy generation performance with a maximum open circuit potential of 0.79 V and a maximum power density output (P_{max}) of $13.5 \mu\text{V}\cdot\text{cm}^{-2}$. Furthermore, it shows a wide LR from 9×10^{-12} – $1 \times 10^{-7} \text{ mol dm}^{-3}$, a low LOD of $3 \times 10^{-12} \text{ mol dm}^{-3}$, and marked selectivity towards ATZ [73]. Compared to ATZ sensors from Table 1, sensors constructed by Salahshoor et al. and Chen et al. showed similar LR and LOD values. It leads us to the conclusion that MIP plasmonic sensors are more sensitive and selective for ATZ detection.

Yola et al. have developed an electrochemical sensor based on a nanocomposite of molecular polymer and platinum nanoparticles (Pt NPs)/carbon nitride nanotubes (C₃N₄ NTs) for the analysis of ATZ. The molecularly imprinted sensor's LR and LOD were calculated to be 1×10^{-12} – $1 \times 10^{-10} \text{ mol dm}^{-3}$ and $1.5 \times 10^{-13} \text{ mol dm}^{-3}$, respectively. This voltammetric sensor, which shows high selectivity and sensitivity, was applied to wastewater samples with a recovery of 96.88–103.70% [74]. Compared to this, MIP plasmonic sensors for the detection of ATZ show a wider range of linearity with a two-orders-of-magnitude higher LOD and a lower percent recovery in real samples. Moreover, Sifiso et al. produced highly fluorescent CdSeTe/ZnS QDs using a conventional organometallic synthesis approach and then encapsulated them with MIPs. As a result, the CdSeTe/ZnS@MIP sensor showed a fast response time of 5 min, while the LOD was $8 \times 10^{-8} \text{ mol dm}^{-3}$. Finally, the sensor was applied to real water samples and showed good recovery values ranging from 92 to 118% [75]. Compared to this fluorescent sensor, MIP plasmonic sensors for ATZ detection presented in Table 1 show a lower LOD by three orders of magnitude, a lower recovery percent in real samples, and the same response time.

To detect ATZ using non-imprinted plasmonic sensors, glass fiber substrates coated with silver nanoparticles were used as SERS plasmonic nanosensors. The LOD of SERS plasmonic substrates for ATZ detection was $1 \times 10^{-12} \text{ mol dm}^{-3}$ [76]. Compared to the data shown in Table 1, this sensor has a similar LOD value, leading to the conclusion that they are sensitive for detecting ATZ.

Albarghouthi et al. reported the construction of a SERS sensor using gold nanorod arrays (AuNR) for fast and sensitive detection of ATZ with an LOD of $1.8 \times 10^{-6} \text{ mol dm}^{-3}$ [77]. Looking at the data shown in Table 1 for the detection of ATZ, we can see that the MIP plasmonic sensors are significantly better in all characteristics, especially in terms of sensitivity, because the LOD is five orders of magnitude lower.

Tang et al. have proposed a highly sensitive and selective method for detecting ATZ using the Raman molecule R6G as a reporter adsorbed on carbon dots (CDs) modified with silver nanoparticles. Under optimal assay conditions, the limit of quantification was estimated to be $1 \times 10^{-8} \text{ mol dm}^{-3}$ with a good LR in the concentration range of 1×10^{-8} – $1 \times 10^{-6} \text{ mol dm}^{-3}$. Determination of ATZ in real water samples was also carried out and showed recoveries ranging from 95% to 117.5% [78]. Unlike the aforementioned sensor, MIP plasmon sensors have narrower LRs, lower LODs and recovery percentages, and high selectivity and sensitivity.

Hierarchical arrays of silver nanoprisms/graphene oxide/silicon nanowires (Ag/GO/SiNWs) as SERS sensors for efficiently detecting ATZ were fabricated by Daoudi et al. High efficiency, high SERS activity, and excellent reproducibility were obtained for the fabricated sensors. Moreover, Ag/GO/SiNWs sensors showed ultrasensitive detection with an LOD of $2 \times 10^{-12} \text{ mol dm}^{-3}$ [79]. These sensors and MIP plasmonic sensors, despite having a difference in LODs of two orders of magnitude, generally show very similar characteristics, making both types of sensors good for ATZ detection.

Supraja et al. have proposed ultrasensitive electrochemical detection of ATZ using electrospun SnO₂ nanofibers. The LOD of ATZ is $9 \times 10^{-22} \text{ mol dm}^{-3}$, in a wide dynamic range of detection that varies from 1×10^{-21} – $1 \times 10^{-6} \text{ mol dm}^{-3}$. In addition, the sensor

exhibits excellent selectivity, reasonable stability (when stored at 4 °C), and good immunity to interference [80]. The electrochemical sensor constructed in this way shows an LOD lower by ten orders of magnitude, as well as a wider LR for ATZ detection compared to MIP plasmonic sensors.

A simple and highly sensitive photoelectrochemical (PEC) aptasensor for ATZ detection was constructed by investigating TiO₂ nanotubes decorated with MoS₂ quantum dots (MoS₂ QDs/TiO₂ NT) as the photoelectrode and aptamer molecules as the recognition element. As a result, the designed PEC aptasensor exhibits high sensitivity and specificity with an LR of $(2\text{--}500) \times 10^{-12} \text{ mol dm}^{-3}$ and an LOD of $9 \times 10^{-13} \text{ mol dm}^{-3}$. Moreover, this PEC aptasensor has been used for the detection of ATZ in real samples of lake water, agricultural wastewater, and sewage water, where the recovery varies from 96–103.6% [81]. Unlike MIP plasmon sensors, the photoelectrochemical aptasensor shows a smaller range of linearity with an LOD lower by two orders of magnitude, which is why the sensors constructed in this way are very sensitive. In addition, the aptasensor shows a higher percentage of recovery, making it possible to apply it to determine ATZ in real samples.

A luminol-H₂O₂ electrochemiluminescence system with AgNPs was used to develop a highly sensitive and specific aptasensor for ATZ detection. The sensor showed good stability, sensitivity, reproducibility, specificity, and excellent recovery in tap water, soil, and cabbage samples in the range of 89.13–123.03%. In addition, the LR for such a sensor is $5 \times 10^{-12}\text{--}4.6 \times 10^{-6} \text{ mol dm}^{-3}$, and the LOD is $2 \times 10^{-12} \text{ mol dm}^{-3}$ [82]. Based on the values shown, it was observed that the sensor has a similar LR, an LOD that is one order of magnitude lower, and a recovery percentage that is significantly higher compared to MIP plasmonic sensors for the detection of ATZ.

From the data discussed above, it is clear that MIP-based plasmonic sensors have great potential to become the most sensitive and selective type of sensors for pesticide detection.

3.2. Pharmaceuticals

Pharmaceuticals are compounds used worldwide to prevent or treat diseases. The global growth of industrialization and urbanization has led to the contamination of the entire ecosystem. Various types of pollutants can affect the environment. Among others, drugs are the focus of attention due to their biological activity. However, protein-based pharmaceuticals are harmless to the environment because they are biodegradable and metabolized by humans. On the other hand, pharmaceutical substances generally are not metabolized and are excreted into the ecosystem through sewage, affecting the health of humans and animals. In addition, drug residues have been observed in the food chain, where they are often present as a mixture of compounds causing acute and chronic toxicity. Toxicity to pharmaceuticals depends not only on exposure time, temperature, and concentration of pharmaceuticals, but also on the species and stage of the organism.

Antibiotics are one of the major discoveries of the last century. They significantly changed the treatment of infections. However, the overuse of antibiotics in human and animal health and agriculture practices causes release into the environment, which is a vector of AMR. Statistically, antibiotics use in animal husbandry is much higher than in human medicine. Antibiotics used in medical and veterinary practice reach the environment through urine and excreta. Shockingly, between 40–90% of the administered antibiotic dose is excreted in the feces and urine as an active form. As a result, they are reaching the environment and contaminating soils, waters, and plants.

AMR is a great public challenge with an important magnitude in the environment that contributes to its evolution and increase [83]. The wastewaters become a reservoir for resistant genes and the development and spread of resistance to pathogens. Environmental monitoring could provide vital information for mitigating the spread of AMR. Therefore, the monitoring of antibiotics in the environment remains a burning issue in the modern world to prevent harmful impacts on aquatic ecosystems and human health due to direct exposure to these synthetic organic compounds.

In addition to antibiotics, non-steroidal anti-inflammatory drugs (NSAIDs) have been identified as a novel class of pollutants due to their overuse and incomplete degradation. They can intrinsically promote abnormal physiological processes and human reproductive damage even at low doses [84]. In addition, their use is connected to increased cancer incidence. NSAIDs are universally present in the environment. The most common NSAIDs are diclofenac, ibuprofen, paracetamol, naproxen, and ketoprofen. Their toxic effects on humans and animals are well-known. Therefore, it is very important to monitor them and help reduce the risk of ecosystem contamination.

Several sensors for pharmaceuticals monitoring employing MIPs and plasmonic detection have been developed. Their overview is given in Table 2.

Table 2. MIP-based plasmonic sensors for pharmaceutical detection and their most important characteristics.

Analyte	Functional Monomer	Sensor Type	Linearity Range [mol dm ⁻³]	Limit of Detection [mol dm ⁻³]	Response Time [min]	Reference
Antibiotics						
Amoxicillin	MAAM	SPR	-	7.3×10^{-11}	-	[85]
Amoxicillin	HEMAGA	SPR	$(2.74\text{--}54.73) \times 10^{-10}$	6×10^{-11}	10	[86]
Amoxicillin	MAA	SPR	$(2.74\text{--}27.37) \times 10^{-10}$	1×10^{-12}	7.5	[87]
Amoxicillin	HEMAGA	SPR	$(2.74\text{--}54.73) \times 10^{-10}$	3×10^{-12}	2.5	[88]
Amikacin	MAAsp	SPR	$(1.7\text{--}25.6) \times 10^{-8}$	4.27×10^{-9}	10	[89]
Ciprofloxacin	MAA	SPR	-	9.69×10^{-9}	5	[90]
Ciprofloxacin	IA	SPR	$1 \times 10^{-13}\text{--}1 \times 10^{-5}$	1×10^{-13}	12.5	[91]
Ciprofloxacin				5.1×10^{-10}		
Moxifloxacin	AA	SPR	-	9.2×10^{-10}	-	[92]
Ofloxacin				1.6×10^{-10}		
Enrofloxacin	bAu@mSiO ₂ @MIP	SERS	$(0\text{--}2.55) \times 10^{-7}$	1.5×10^{-9}	-	[93]
Enrofloxacin	Dopamine	LSPR	$(6.96\text{--}278.24) \times 10^{-8}$	1.7×10^{-7}	1.5	[94]
Erythromycin	MAA	SPR	$(6.8\text{--}68.1) \times 10^{-6}$	4×10^{-7}	3	[95]
Kanamycin	4-					
Kanamycin	vinylbenzeneboronic acid	SPR	$1 \times 10^{-7}\text{--}1 \times 10^{-5}$	1.2×10^{-8}	-	[96]
Oxytetracycline	MAA	SPR	$(1\text{--}30) \times 10^{-8}$	8.1×10^{-9}	15	[97]
Oxytetracycline hydrochloride						
Tetracycline hydrochloride	AM and AA	SPR	$(0\text{--}9.6) \times 10^{-7}$	-	Fast response	[98]
Penicillin G	MAPA and MAC	SPR	$(3\text{--}2990) \times 10^{-9}$	-	1	[99]
Spiramycin	AM	SERS	$(1\text{--}200) \times 10^{-10}$	2.7×10^{-11}	-	[100]
Tetracycline	MAA and IA	SPR	$1 \times 10^{-13}\text{--}1 \times 10^{-7}$	1.38×10^{-14}	15	[101]
Tetracycline	AM and AA	SPR	$10^{-8}\text{--}10^{-5}$	2.2×10^{-9}	Fast response	[102]
Vancomycin	IA	SPR	$(6.9\text{--}690) \times 10^{-9}$	2.83×10^{-9}	1.5	[103]
Other pharmaceuticals						
Andarine				8.4×10^{-10}		
Ligandrol	NIPAm, NAPA, BIS, and AA	SPR	-	6.9×10^{-10}	-	[104]
RAD-140				7.0×10^{-10}		
Cocaine	AM	SPR	$(6.6\text{--}32.97) \times 10^{-10}$	3.3×10^{-9}	17	[105]
Etoposide	HEMA-MAGA	LSPR	$1.7 \times 10^{-12}\text{--}1.7 \times 10^{-9}$	4.25×10^{-13}	10	[106]
Paracetamol	MAA	SERS	$(3.3\text{--}5.3) \times 10^{-7}$	3×10^{-7}	-	[107]
Propranolol	MAA	SERS	$1 \times 10^{-11}\text{--}1 \times 10^{-4}$	1×10^{-11}	-	[108]
Tryptamine	MAA	SERS	$1 \times 10^{-6}\text{--}1 \times 10^{-2}$	4.85×10^{-7}	-	[109]
Theophylline	MAA	SPR	$10^{-6}\text{--}10^{-4}$	1×10^{-6}	10	[110]

NIPAm—nisopropylacrylamide; NAPA—N-(3-aminopropyl) methacrylamide hydrochloride; BIS—N, N0-methylenebisacrylamide; AA—acrylic acid; AM—acrylamide; MAA—methacrylic acid; bAu@mSiO₂@MIP—multi-branched gold-silica-molecularly imprinted polymer; MAAM—methacrylamide; MAPA—N-methacryloyl-l-phenylalanine; MAC—N-methacryloyl-(L)-cysteine methyl ester; HEMAGA—2-hydroxyethyl-methacrylate-methacryloyl-amidoglutamic acid; MAAsp—methacryloylamidoaspartic acid; IA—itaconic acid; HEMA-MAGA—2-hydroxyethyl methacrylate methacryloylamidoglutamic acid.

As can be seen from Table 2, most pharmaceutical MIP-based plasmonic sensors available in the literature nowadays are for antibiotics detection. AM, AA, and MAA are functional monomers usually used for MIP synthesis. In most cases, the methods used for the detection are SPR, LSPR, and SERS. All sensors presented in Table 2 are highly selective, with a wide LR and low LOD. Some of them need a few minutes for the analysis, but most require longer periods for detection (10 to 20 min). We aim to discuss the characteristics of the amoxicillin (AMO) sensors presented in Table 2 compared to the other types of sensors available for the same pollutant.

A highly selective and sensitive photoluminescent probe for the detection of AMO was constructed using a sol-gel process with 3-aminopropylethoxysilane as a functional monomer, tetraethoxysilane as a cross-linker, and AMO as a template molecule. Under optimal conditions, the LR is from 5.5×10^{-10} – 1.4×10^{-7} mol dm⁻³, and the LOD is 3.83×10^{-10} mol dm⁻³. The developed method showed good repeatability and reproducibility, achieving a satisfactory recovery of 85–102% [111]. According to Table 2, it was observed that MIP plasmonic sensors for the detection of AMO, compared to the previously described sensor, have a slightly wider LR of the same order of magnitude with an LOD that is lower by two orders of magnitude.

Lee et al. have developed a sensor based on MIPs for the detection of AMO based on two modes of detection (fluorescence and electrochemiluminescence) and dual recognition. Fluorescence and electrochemiluminescence modes have detection ranges of $(5\text{--}1000) \times 10^{-11}$ mol dm⁻³ and $(5\text{--}1500) \times 10^{-11}$ mol dm⁻³, respectively, with LODs of 9.2×10^{-12} mol dm⁻³ and 8.3×10^{-12} mol dm⁻³, respectively. A sensor constructed in this way provides increased sensitivity, selectivity, and accuracy. In addition, it can be used to detect AMO in real samples, where the fluorescence detection mode gave a recovery of 88.90–105.20%, while the electrochemiluminescence detection mode showed a recovery of 88.60–106.60% [112]. Comparing the performance of the MIP plasmonic sensors with the constructed dual sensor, it was observed that the MIP sensors have a wider range of linearity, while both types of sensors have an LOD of the same order of magnitude, which means that they are very sensitive for detecting AMO.

Next, a molecularly imprinted electrochemical aptasensor was constructed based on the co-deposition of zinc oxide and gold nanoparticles/reduced graphene oxide composite. For the obtained sensor, the LR was from 1×10^{-14} – 1×10^{-8} mol dm⁻³ and the LOD was 3.3×10^{-15} mol dm⁻³. The sensor showed satisfactory selectivity, reproducibility, and stability, and was successfully used to determine 1×10^{-9} mol dm⁻³ of AMO in real water and food samples [113]. The observed electrochemical aptasensor, compared to the sensors shown in Table 2, offers a slightly narrower LR and high sensitivity for detection due to a lower LOD by three orders of magnitude.

A specific form of SERS sensors was developed by Wail et al. An efficient detection process for ultra-low concentration of AMO in the range of 1×10^{-10} – 1×10^{-4} mol dm⁻³ was achieved [114]. Sensors constructed in this way show a wider LR than those in Table 2.

A highly sensitive Ag dendrite-based microfluidic-SERS sensor was fabricated by an electrogalvanic displacement reaction between Ag and Cu. The LOD was 2.7×10^{-9} mol dm⁻³ [115]. MIP plasmonic sensors for AMO detection were observed to perform better with an LOD lower by three orders of magnitude.

Scientists also developed a dual-mode colorimetric and SERS platform for the detection of AMO using electrochemically synthesized copper nanoparticles (CuNPs) and copper-graphene oxide (Cu-GO) nanocomposites. The Cu-GO-based colorimetric nanosensor shows high sensitivity to AMO in the LR $(5\text{--}50) \times 10^{-6}$ mol dm⁻³ with an LOD of 1.71×10^{-6} mol dm⁻³, which is 1.3 times lower than the CuNPs-based colorimetric nanosensor (2.17×10^{-6} mol dm⁻³). More interestingly, the Cu-GO-based SERS nanosensor has an LR of 1×10^{-8} – 1×10^{-3} mol dm⁻³ and an LOD value of 1.2×10^{-9} mol dm⁻³, which is 13 times lower than the CuNPs-based SERS sensor (1.52×10^{-7} mol dm⁻³). The dual optical nanosensors developed in this way have shown good practical applicability for AMO detection in real tap water samples with a recovery of about 95% [116]. In contrast to MIP

plasmonic sensors, the formed dual optical nanosensors show four-orders-of-magnitude higher LR and five-orders-of-magnitude higher LOD, with a lower percent recovery for the determination of AMO in real samples.

The development of a colorimetric sensor based on silver nanoparticles coated with quercetagenin (Qt AgNPs) for the detection of AMO was reported. The LR of the formed sensor is $(1-9.5) \times 10^{-5} \text{ mol dm}^{-3}$. The LOD is $4.46 \times 10^{-6} \text{ mol dm}^{-3}$ [117]. It is obvious that MIP plasmonic-based sensors have a smaller range of linearity. Still, a higher LOD by six orders of magnitude leads to the conclusion that they are significantly more sensitive for the detection of AMO.

An impedimetric aptasensor was fabricated by the synergy between functionalized TiO_2 materials and gold nanoparticles. Under optimal conditions, the sensor successfully detected AMO in the $(5-30) \times 10^{-10} \text{ mol dm}^{-3}$ range and reached an LOD of $2 \times 10^{-10} \text{ mol dm}^{-3}$. The sensor shows good selectivity, reproducibility, and stability with a recovery of 91.6–110.3% [118]. The impedimetric aptasensor shows a narrower range of linearity compared to MIP plasmonic-based sensors as well as a higher LOD by two orders of magnitude, and the percentage of recovery in real samples is higher.

3.3. Microorganisms

The presence of microorganisms and their toxins in drinking water and water environments may increase potential human health risks. Microbial contamination implies a release of microorganisms into the environment, originating mainly from waste products. Microbial pollution is a serious issue because it can lead to many health problems, diseases, and death. In addition, exposure to pathogens also creates an economic impact that can be devastating [119]. Microorganisms causing contamination of the environment mainly include bacteria, bacterial toxins, protists, and viruses. It is important to notice that viruses do not metabolize without their hosts, unlike bacteria, which reproduce and do things on their own [120].

Humans and animals use great amounts of water, often in contact with communal or other types of waste. Used water travels back into the water cycle and out into the oceans. As a result, human safety is endangered, but degrading the habitats in natural systems has also become a great concern [120]. Water-borne diseases caused by various microorganisms have been the causes of many outbreaks [121,122]. Those diseases are mainly a problem in developing countries, but also represent a serious challenge in developed countries. Pathogen contamination is a leading cause of impairment caused by pathogens originating from water resources [122].

Aflatoxin B1 (AFB1) is known as the most toxic mycotoxin, originating from host crops infected by some species of *Aspergillus*. It can be transferred to water easily. Through communal waste, AFB1 is spread into the environment. It is a genotoxic, carcinogenic, and immunosuppressive substance that causes acute and chronic toxicity issues. Associated health problems are difficult to diagnose due to AFB1 omnipresence and long-term exposure to it [123]. The International Agency for Research on Cancer has classified AFB1 as a human carcinogen belonging to Group 1 [124].

Salmonella is usually connected to the pathogens causing foodborne diseases. Still, its presence and persistence have also been reported in surface waters. It includes rivers, lakes, and ponds, while groundwater generally is of better microbial quality. *Salmonella* species (*Salmonella* spp.) can be found almost everywhere. They can create serious complications, including diarrhea, enteritis, and even death. *Salmonella* spp. are classified as zoonotic agents [125].

Traditional methods of bacterial counts are tiring and slow, so new techniques have to be developed. As mentioned, the use of MIPs as a recognition unit provides high selectivity to a sensor, and the use of plasmonic effects for detection provides better characteristics of the sensor, mainly by lowering the LOD and rapidness. Therefore, it makes them a great choice for sensor components employed in environmental protection. MIP SPR sensors

for the detection of microorganisms and their toxins are shown in Table 3, along with their characteristics.

Table 3. MIP plasmonic sensors for the detection of microorganisms and their toxins.

Analyte	Functional Monomer	Sensor Type	Linearity Range [mol dm ⁻³]	Limit of Detection [mol dm ⁻³]	Response Time [min]	Reference
Toxins						
Ochratoxin A	MAPA and HEMA	SPR	$(2.5\text{--}495) \times 10^{-7}$ mol dm ⁻³	7×10^{-8} mol dm ⁻³	3.5	[126]
aflatoxin B1	MIP film	SEF	$(9.6\text{--}800) \times 10^{-7}$ mol dm ⁻³	9.6×10^{-7} mol dm ⁻³	-	[127]
aflatoxin B1	MAPA	SPR	$(3.2\text{--}3200) \times 10^{-7}$ mol dm ⁻³	3.3×10^{-9} mol dm ⁻³	3.5	[128]
aflatoxin M1	MAPA	SPR	$(9.1\text{--}6100) \times 10^{-10}$ mol dm ⁻³	1.21×10^{-9} mol dm ⁻³	3.5	[129]
Endotoxin	HEMA-MAH	SPR	$(9.6\text{--}1914) \times 10^{-10}$ mol dm ⁻³	4.4×10^{-10} mol dm ⁻³	3.5	[130]
Zearalenone	Pyrrole	SPR	$(9.4\text{--}942.5) \times 10^{-7}$ mol dm ⁻³	9.4×10^{-7} mol dm ⁻³	10	[131]
mycoestrogen	Pyrrole	SPR	$3.4 \times 10^{-7}\text{--}3.4 \times 10^{-4}$	$<3.4 \times 10^{-7}$	20	[132]
Deoxynivalenol	Pyrrole	SPR				
Microorganisms						
Enterococcus faecalis	MAH	SPR	$2 \times 10^4\text{--}1 \times 10^8$ CFU cm ⁻³	1.05×10^2 CFU cm ⁻³	0.75	[133]
Salmonella paratyphi	MAH	SPR	$(2.5\text{--}15) \times 10^6$ CFU cm ⁻³	1.4×10^6 CFU cm ⁻³	3.5	[134]
Escherichia coli	MAH	SPR	$1.5 \times 10^1\text{--}1.5 \times 10^6$ CFU cm ⁻³	0.57 CFU cm ⁻³	20 min	[135]
T4 bacteriophage	PVA	SPR	$1 \times 10^4\text{--}4 \times 10^6$ PFU mL ⁻¹	6×10^3 PFU mL ⁻¹	3.5	[136]

MAPA—N-methacryloyl-L-phenylalanine; HEMA—2-hydroxyethyl methacrylate; HEMA-MAH—2-hydroxyethyl methacrylate-N-methacryloyl-(L)-histidine methyl ester; MAH—N-methacryloyl-(L)-histidine methyl ester; PVA—polyvinyl alcohol.

As can be noticed from Table 3, all listed sensors are highly sensitive and selective for certain microorganisms or toxins, which is one of the biggest advantages of MIP sensors. Most of the sensors from this group are developed for AFB1, *Salmonella*, and *Escherichia* detection. In addition, most of them have quick response times, around 200s, but some require up to 20 min for the analysis. Functional monomers used are MAPA, MAH, and pyrrole. The method dominantly used for the detection is SPR.

In the literature, many sensors for detecting microorganisms and their toxins can be found: conventional, using MIP as a recognition element but not plasmonic, and plasmonic but not MIP. The many types of sensors developed for AFB1 allowed us to compare the contribution of individual components.

Guo et al., in their work, described a fluorometric, aptamer-based assay for its detection. In the presence of humic acid, aptamer-modified carbon dots fluorescence is quenched. By adding aflatoxin B1, DNA-CDs detach from humic acid, restoring the fluorescence. This type of detection had a narrow LR $(3.2\text{--}25.6) \times 10^{-7}$ mol dm⁻³, but the LOD was low $(2.2 \times 10^{-7}$ mol dm⁻³) [137]. Moreover, Sun et al. constructed a rapid and sensitive aptamer-based SPR sensor for AFB1 detection. The sensor showed remarkable performance in the wide LR of $4 \times 10^{-10}\text{--}2 \times 10^{-7}$ mol dm⁻³ with an LOD of 4×10^{-10} mol dm⁻³ and a response time of 120s [138]. On the other hand, Sergeyeva et al. constructed a smartphone-based fluorimetric sensor using MIP as a recognition unit. Functional monomers were acrylamide and 2-acrylamido-2-methyl-1-propanesulfonic acid. Introducing an MIP resulted in a widening LR compared with the work of Guo et al. $((6.4\text{--}32) \times 10^{-5}$ mol dm⁻³), and increasing selectivity but also increasing the LOD around 200 times $(4.8 \times 10^{-5}$ mol dm⁻³) [139].

Sergeyeva et al. later constructed an MIP plasmon-enhanced fluorescence sensor for AFB1 detection, which had better characteristics than a fluorescent one (Table 3). The MIP film provided selective binding of AFB1, and sensitivity was increased by enhancing the fluorescent signal of the analyte molecule by the local electric field induced close to the surface of silver nanoparticles excited at the LSPR wavelength. The results showed that this sensor could detect AFB1 in a wide LR with an LOD as low as $9.6 \times 10^{-7} \text{ mol dm}^{-3}$ [127]. An MIP SPR sensor for the detection of AFB1 with the widest LR (3.2×10^{-10} – $3.2 \times 10^{-5} \text{ mol dm}^{-3}$) and LOD of $3.3 \times 10^{-9} \text{ mol dm}^{-3}$ was constructed by Akgonullu et al. [128]. The sensor showed remarkable characteristics in comparison with all other detection methods for AFB1 (Table 3).

A highly selective and sensitive MIP SPR sensor for *E. coli* was constructed by Ozgur et al. with an incredible LOD as low as 0.57 CFU cm^{-3} (Table 3). It is far lower than LODs reported by other researchers, but the response time was 20 min. [135]. Si et al. reached an LOD of $3 \times 10^5 \text{ CFU cm}^{-3}$ and a response time of 5 min by using a dextran-modified sensor chip [140], while Yaseen et al. reported an MIP electrochemical chemosensor for the detection of *E. coli* with an LOD of $2.9 \times 10^4 \text{ CFU cm}^{-3}$ and detection time of 60 min [141]. Comparing these sensors, we can conclude that using the MIP SPR sensor reported by Ozgur et al. brings high selectivity and sensitivity but takes time to detect *E. coli*. On the other hand, the sensor reported by Si et al. is not as sensitive as the previous one but has a faster response.

3.4. Metals

Industrial wastewaters commonly contain heavy metals such as mercury, copper, cadmium, zinc, chromium, lead, and nickel. They can be highly toxic for many organisms. Some are essential to human health, as they are a component of many proteins. For example, copper is known to be a cofactor of many enzymes. Yet, in the human body, excess of copper can lead to copper poisoning, a type of metal poisoning. Acute symptoms are mostly connected to gastrointestinal problems, while long-term copper exposure can damage the liver and kidneys [142]. Zinc is known as relatively nontoxic. Still, it can be toxic to humans when in high dosage. Manifestations of zinc toxicity are mainly gastrointestinal symptoms such as nausea, vomiting, and epigastric pain, but also lethargy and fatigue [143]. On the other hand, the toxicity of mercury and cadmium is well known. The harmful effects of mercury are mainly acute and include the action on the nervous, digestive, and immune systems and lungs and kidneys, and may be fatal [144]. Alternatively, the effects of cadmium poisoning mostly have long-term consequences because this metal causes mutations and chromosomal deletions, increasing the chances of cancer development [145].

Although the conventional methods for heavy metal ion detection have low LODs, they are time-consuming, the equipment is expensive, samples often require pre-treatment, and the dynamic range could be narrow. Compared to other analytical methods, plasmonic sensors show faster determination of heavy metals in tap and natural water, making them suitable for wastewater treatment monitoring [146]. Imprinting metal particles to polymers highly increases the selectivity of the sensor. As the metal ions are used for impregnation, the resulting product is called an ion-impregnated polymer (IIP).

Sensors that combine polymer imprinting and plasmon resonance are developed to achieve high sensitivity, rapidness, wide LRs, and low LODs. Ion-impregnated plasmonic sensors for detecting heavy metals and their characteristics are shown in Table 4.

As can be noticed from Table 4, MIP-based plasmonic sensors are available for just a few metals, namely copper, mercury, cadmium, and zinc. They all have quick response times, from 20s to a few minutes. Functional monomers used are HEMAC, MAC, and PVA. Methods mainly used for the detection are SPR and LSPR.

Table 4. Ion-impregnated plasmonic sensor for detection of metals.

Analyte	Functional Monomer	Sensor Type	Linearity Range [mol dm ⁻³]	Limit of Detection [mol dm ⁻³]	Response Time [min]	Reference
Cu ²⁺	HEMAC	SPR	(1–25) × 10 ⁻¹⁰	1 × 10 ⁻¹⁰	Rapid	[147]
Cu ²⁺	MAC	SPR	(4–500) × 10 ⁻⁸	2.7 × 10 ⁻⁸	0.3	[148]
Hg ²⁺	PVA	SPR	(4–5440) × 10 ⁻⁹	4 × 10 ⁻⁹	2	[149]
Hg ²⁺	PVA	LSPR	(0–2.5) × 10 ⁻⁷	1 × 10 ⁻⁷	-	[150]
Cd ²⁺	MAC	SPR	(9–4500) × 10 ⁻⁷	9 × 10 ⁻⁸	1.5	[151]
Zn ²⁺	HEMAH	SPR	(7.5–15) × 10 ⁻⁶	2.9 × 10 ⁻⁶	8	[152]

HEMAC—hydroxyethyl methacrylate-*N*-methacryloyl-(*L*)-cysteine methyl ester; MAC—*N*-methacryloyl-*L*-cysteine methyl ester; PVA—polyvinyl alcohol; HEMAH—2-hydroxyethyl Methacrylate-*N*-methacryloyl-(*L*)-histidine methyl ester.

Other sensors for detecting metals can be found in the literature: conventional, using IIP as a recognition element, and plasmonic. D'Ilio et al. used ICP MS to detect heavy metals, and results showed that the LOD for Ar, Cd, Cr, and Pb is as low as 7.1×10^{-10} mol dm⁻³ for Cd²⁺ ions and a little higher for others, but LR is narrow $(1.1\text{--}13) \times 10^{-9}$ mol dm⁻³ [153]. As this method is demanding, SPR sensors have been developed for metal determination. Yi and Shu developed a sensitive and selective SPR sensor for Cd²⁺ ions in lake water by functionalizing Au nanoparticles with di-(1*H*-pyrrol-2-yl) methanetione. Due to the aggregation in the presence of Cd²⁺ ions, the color change from red to blue can be observed with the LR $(5\text{--}160) \times 10^{-7}$ mol dm⁻³ and LOD 1.66×10^{-8} mol dm⁻³ [154]. Deymehkar et al. modified Au nanoparticles with kryptofix (1,7-diaza-15-crown-5) to create an SPR sensor for Cu²⁺ ions. The sensor detects Cu²⁺ ions due to the formation of a sandwich between two 1,7-diaza-15-crown-5 moieties attached to different nanoparticles and Cu²⁺ ions, resulting in surface plasmon adsorption band red shift. The LOD reported in this work is 2×10^{-7} mol dm⁻³ [155]. Introducing ion imprinting polymers as recognition units results in higher selectivity, but LR and LOD vary depending on the detection technique and functional monomer used.

Hu et al. reported a highly selective IIP chemiresistor sensor using functionalized reduced graphene oxide to detect Cd²⁺. The functional monomers used were polyethyleneimine and methacrylic acid. The prepared sensor showed remarkable performance in the LR of $1.8 \times 10^{-8}\text{--}1.8 \times 10^{-5}$ mol dm⁻³, and the LOD achieved was 8×10^{-9} mol dm⁻³. The proposed sensor is highly sensitive and can be reusable [156].

A quartz crystal microbalance IIP sensor was proposed for detecting Cu²⁺ ions using *N*-methacryloyl-*L* histidine methyl ester as a functional monomer by Aydogan et al. With this sensor, the detection was rapid and selective, and the LOD was 4.07×10^{-8} mol dm⁻³ [157].

Gerdan et al. designed an IIP SPR sensor for Cu²⁺ detection using *N*-methacryloyl-*L*-cysteine methyl ester as a functional monomer on a gold surface. The sensor had a wide LR, but the LOD was not so high [148]. With the use of a different functional monomer, the LR narrows, but the LOD is lower by 270 times [147]. Compared with the other mentioned sensors for Cu²⁺ detection, the latter showed remarkable characteristics. The IIP SPR sensor showed 4000 times lower LOD in the case of Hg²⁺ compared with the same components of the IIP LSPR sensor. The non-IIP SPR sensor for detecting Cd²⁺ ions has given the best LR and LOD results, as LOD is nearly eight times lower than in the IIP SPR one. It could maybe be improved by using some other functional monomer.

In summary, using IIP as a recognition unit and plasmonic effects for the detection of metals largely improves sensor characteristics and allows faster and more selective detection of metals of interest.

3.5. Endocrine Disruptors

Endocrine disruptors are chemicals in the environment, food sources, personal care products, and manufactured products that mimic or interfere with the body's hormones. They can be both natural and man-made. EDs can cause many complications in the human organism, including developmental malformations, disturbances in the immune and nervous system function, reproductive, and other problems. Those chemicals are present in numerous everyday products, such as plastic containers, metal food cans, detergents, flame retardants, food, toys, cosmetics, and pesticides. As such, they represent a ubiquitous threat to the human organism. Some of the most notorious examples are bisphenol A (BPA) and hormones and their analogs.

Bisphenol A is an industrial component used mainly as a monomer in the production of polymers. In addition, it can be used as an antioxidant in some plasticizers or as a polymerization inhibitor of polyvinyl chloride (PVC) [158,159]. BPA can be found in many materials used for food packing and children's products. Due to plastics' mass production and extensive applications, the presence of BPA is inevitable in the environment. It is proven to be highly toxic. BPA is most notorious as an endocrine disruptor [159–161]. BPA exposure during the perinatal period may influence prostate and mammary gland development, causing anxiety and changes in brain biochemical signaling in different potentially significant brain regions. BPA's effects on neurogenesis, gene expression, the neuroendocrine system, and the morphology of certain brain regions are indicated in many studies [162]. Moreover, it has been shown that BPA could induce carcinogenesis and mutagenesis [163]. In 2011, the European Union banned BPA use in polycarbonate baby bottle production due to its high toxicity [159].

The presence of hormones in the environment and food is a big problem, as they can disrupt the function of the endocrine system and its physiological functions such as growth, development, and reproduction [164]. Even a subtle change in the concentration of hormones in the organism may cause problems, and that is why their detection is very important and requires that the LOD is low [165].

In Table 5, MIP plasmonic sensors used for hormone detection available in the literature are presented.

Table 5. MIP plasmonic sensors for hormone detection.

Analyte	Functional Monomer	Sensor Type	Linearity Range [mol dm ⁻³]	Limit of Detection [mol dm ⁻³]	Response Time [min]	Reference
Testosterone	MAA and HEMA	SPR	3.47×10^{-12} – 3.5×10^{-7}	3.47×10^{-12}	12	[166]
Testosterone	MAA	SPR	1×10^{-12} – 1×10^{-8}	1×10^{-12}	1.5	[167]
Testosterone	HEMA-MAA	SPR	$(1.73$ – $69.34) \times 10^{-6}$	1.32×10^{-6}		[168]
Progesterone	IA	SPR	1×10^{-18} – 1×10^{-8}	0.28×10^{-19}	10	[169]
Progesterone	MAA	SPR	1×10^{-16} – 1×10^{-6}	1×10^{-16}	16	[170]
17 beta-estradiol	MALM	SPR	7.3×10^{-5} – 3.7×10^{-2}	7.3×10^{-5}	0.16	[171]
17 beta-estradiol	HEMA-MAA	SPR	2.5×10^{-16} – 2.5×10^{-8}	9.14×10^{-18}	2.5	[172]
Gonadorelin	Norepinephrine	SPR	$(4.2$ – $135) \times 10^{-10}$	5.2×10^{-11}	1.5	[173]

MAA—methacrylic acid; HEMA—2-hydroxyethyl methacrylate; IA—itaconic acid; MALM—N-methacryloyl-L-leucine methyl ester.

MIP SPR sensors for testosterone detection constructed by Zhang et al. [166], Tan et al. [167], and Cimen et al. [168] are all highly selective for testosterone due to the MIP recognizing unit and have LODs of 3.47×10^{-12} , 1×10^{-12} , and 1.3×10^{-7} mol dm⁻³, respectively. The Zhang et al. sensor presented a wider LR than the one constructed by Tan et al., but the LOD and response time went in favor of the Tan et al. sensor. They were all tested for the detection of testosterone in real samples, where they showed not-so-different characteristics. Yockell-Lelièvre et al. compared SPR and LSPR non-MIP sensors for the detection of testosterone [174]. The SPR sensor was based on a thin gold film on the dove prism, and the LSPR sensor was based on a monolayer of Au nanoparticles on the dove prism. Anti-testosterone was immobilized on the surface of the sensors. Results

showed that the sensitivity of the SPR sensor was $1.03 \times 10^{-9} \text{ mol dm}^{-3}$, and of the LSPR was $8.9 \times 10^{-11} \text{ mol dm}^{-3}$, both higher than the sensors reported by Zhang et al. and Tan et al.

An MIP EIS sensor for testosterone was reported by Liu et al. [175]. The functional monomer used in this research was o-phenylenediamine, and the GO/MIP composite was made by electrochemically grafting MIP on the graphene oxide sheet-modified electrode. The nanosheet structure and the high surface area of GO contributed to the very high sensitivity of this sensor. The LOD of this sensor was $4 \times 10^{-16} \text{ mol dm}^{-3}$, lower than previously mentioned.

Nawaz et al. reported a highly sensitive, selective, and rapid MIP SPR sensor for progesterone detection using itaconic acid as a functional monomer [169]. The characteristics of this sensor were remarkable: wide LR, selectivity, reusability, rapidness, and sensitivity. By the report, this sensor could detect progesterone in tap water, lake water, and human saliva in 600 s in the range of 1×10^{-18} – $1 \times 10^{-8} \text{ mol dm}^{-3}$ and an LOD of $2.8 \times 10^{-20} \text{ mol dm}^{-3}$, far lower than the MIP SPR sensor reported by Yu et al. ($1 \times 10^{-16} \text{ mol dm}^{-3}$), which used methacrylic acid as a functional monomer. Other sensors found in the literature had significantly higher LODs than the presented MIP SPR ones [176,177].

A 17β -estradiol MIP SPR sensor, based on 2-hydroxyethyl methacrylate-methacrylic acid as a functional monomer, reported by Jiao et al., also showed remarkably better performances than others found in the literature, as it could detect 17β -estradiol at the concentration of $9.14 \times 10^{-18} \text{ mol dm}^{-3}$ in tap water and human urine in only 150 s [172,178,179].

A significant subclass of EDs based on research performed on MIP plasmonic detection is BPA, as many research articles have been published regarding this theme. Table 6 presents reported MIP plasmonic sensors and their characteristics for BPA detection.

Table 6. MIP plasmonic sensors for BPA detection and their characteristics.

Analyte	Functional Monomer	Sensor Type	Linearity Range [mol dm^{-3}]	Limit of Detection [mol dm^{-3}]	Response Time [min]	Reference
BPA*	EGDMA-VIM	SPR	$(3.5\text{--}438) \times 10^{-7}$	8.7×10^{-8}	5	[180]
	4VP	SPR	$(1\text{--}100) \times 10^{-8}$	6.84×10^{-9}		[181]
	MAA	SERS	$(3\text{--}1000) \times 10^{-7}$	5×10^{-8}	20	[182]
	MIP NPs	LSPR		$<1 \times 10^{-9}$		[183]
	Triethoxysilane	SERS	$(2.5\text{--}100) \times 10^{-6}$	5×10^{-7}		[184]

BPA*—bisphenol A; EGDMA-VIM—ethylene glycol dimethacrylate-*N*-methacryloyl-L-phenylalanine-vinyl imidazole; 4VP—4-vinyl pyridine; MAA—methacrylic acid.

As can be noticed in Table 6, all of the reported sensors are sensitive, selective, and reusable, but the LRs, LODs and response times vary regarding sensor type and functional monomer used. Shaik et al. [180] and Zhu et al. [181] both constructed an SPR sensor but used a different functional monomer as a recognition unit. Comparing their features, the sensor reported by Zhu et al. has around a ten times lower LOD than the sensor reported by Shaik et al., but, in the combination of these two, an LR of 1×10^{-8} – $4.38 \times 10^{-5} \text{ mol dm}^{-3}$ could be achieved. Similarly, Wang et al. [182] and Xue et al. [184] constructed MIP SERS sensors for the detection of BPA using different functional monomers. The sensor reported by Wang et al., using MAA as a functional monomer, showed better performances, as it had a wider LR (3×10^{-7} – $1 \times 10^{-4} \text{ mol dm}^{-3}$ compared to 2.5×10^{-6} – $1 \times 10^{-4} \text{ mol dm}^{-3}$) and a ten times lower LOD. The best performances of the reported MIP plasmonic sensors presented in the table was the MIP LSPR sensor reported by Uchida et al., as it was able to detect BPA in concentrations lower than $1 \times 10^{-9} \text{ mol dm}^{-3}$ [183]. All of the reported sensors were successfully tested on real samples.

Compared with the other sensors found in the literature, these sensors had very good characteristics. Hegnerova et al. reported an SPR sensor based on the detection of the unreacted anti-BPA after incubation with BPA. The LR was wide, at 4.38×10^{-7} – 4.38×10^{-3} mol dm⁻³, but the LOD was 3.5×10^{-7} mol dm⁻³, higher than MIP plasmonic sensors, and the time required for the analysis was 210 min [185]. A multi-walled carbon nanotube-based MIP was developed and used for the modification of glassy carbon electrodes in order to electrochemically detect BPA by Anirudhan et al. Even though the LOD of BPA using this sensor is lower than any presented here (2×10^{-11} mol dm⁻³), the LR is very wide, ranging from 1×10^{-10} – 4×10^{-4} mol dm⁻³, which makes the use of this sensor very specific [186].

3.6. Polycyclic Aromatic Hydrocarbons

Polycyclic aromatic hydrocarbons are persistent pollutants that contain two or more fused aromatic rings. PAHs most frequently found in the environment contain two to seven fused benzene rings. Detection and remediation of PAHs from the environment have been a global concern due to their wide range of biological toxicity. Because of their abundant discharge from anthropogenic sources, PAHs are omnipresent in aquatic and terrestrial ecosystems and the atmosphere [187,188]. The main anthropogenic activities contributing to PAH emissions are incomplete combustions in various industrial processes, such as coal gasification, waste burning, iron, aluminum, cement, rubber tire, fungicide, insecticide, and steel production, dye manufacturing, asphalt industries, exhaust from refineries, and power production [187,189–193]. There are also mobile emission sources, which include exhaust from aircraft, ships, and trains [187,189,190]. In addition to anthropogenic emission sources, there are natural emission sources of PAHs [187,193]. Some of them are volcanic eruptions and natural forest fires, but their contribution is negligible compared to anthropogenic activities [187,189–191].

Not all PAHs have the same effects on animal health [187,194]. Most are mutagenic, carcinogenic, teratogenic, and immunotoxic [187,194–196]. Acute toxic effects of PAHs consist of skin and eye irritation, vomiting, diarrhea, confusion, and inflammation [187,191]. On the other hand, chronic health effects comprise kidney and liver damage, decreased immune function, and lung failure [187,191]. PAHs are phototoxic [187,197]. They absorb UVA light, and, due to that, reactive species form in the cells. Reactive species can damage cell membranes, nucleic acid, and proteins [187,197,198]. PAHs are also genotoxic and carcinogenic. In a mammalian organism, they are mainly detoxified by cytochrome P450 [187,191,198]. Nevertheless, the metabolism of some PAHs also generates reactive intermediates capable of damage generation and genotoxic effects exertion [187,191]. According to the International Agency for Research on Cancer (IARC), PAHs are categorized into groups 1 (carcinogenic to humans), 2A (probably carcinogenic to humans), 2B (possibly carcinogenic to humans), and 3 (not classifiable as carcinogenic to humans) [187,199]. Organs prone to tumor formation due to long-term exposure to PAHs are the lungs, skin, esophagus, colon, pancreas, bladder, and women's breasts [187,198,200]. PAHs are teratogenic and can induce human reproductive system abnormalities. They act as antiestrogens and antiandrogens by directly binding with estrogen and androgen receptors [187,196]. PAH exposure could lead to changes in sperm quality, testicular function, and egg viability, and DNA damage in oocytes, ovarian damage, polycystic ovary syndrome, fertility issues, spontaneous abortion, and premature birth [187,196]. Prenatal exposure to a high concentration of PAHs is connected to a low IQ and behavioral problems in the early-age child and childhood asthma [187,194,201]. Immunotoxicity of PAHs is also documented. They can cause the inhibition of pre-B, pre-T, and myeloid cell development, B and T cell suppression, apoptosis of lymphoid tissues, disruption of myelopoiesis, and altered cytokine production by macrophages and monocytes [187,194,195,202]. Exposure to PAHs induces structural and functional changes in bone marrow, affecting the whole immune system [187,203]. Still, the PAH concentrations required to induce immunotoxicity are higher than those needed to generate cancer [187,195].

The standard methods for the detection of PAHs, comprising gas chromatography, high-performance liquid chromatography, mass spectrometry, and electrophoresis, require expensive and sophisticated equipment, large sample volume, and complicated sample preparation, prolonging the time for obtaining results and possible action [204,205]. Furthermore, these methods use large amounts of organic solvents, which are also toxic to the environment. The limitation of these methods led to the development of other instrumental techniques, such as SERS and fluorescence spectrophotometry, which are considered rapid, non-destructive, highly sensitive, and selective techniques for detecting PAHs in real samples [206,207].

Castro-Grijalba et al. developed the only currently available hybrid plasmonic SERS-based MIP sensor to determine PAHs [208]. MIP substrate has been fabricated based on the layer-by-layer deposition of gold nanoparticles (AuNPs), which were polymerized with methacrylic acid (MAA) as a monomer and pyrene or fluoranthene as analyte/template molecules (Au@MIP substrate). Along with the Au@MIP substrate, the non-imprinted plasmonic substrate (Au@NIP) was produced in the same way except for template molecules. The SERS detection was performed under the excitation of a 785 nm laser for both pyrene-based and fluoranthene-based Au@MIP and Au@NIP substrates. The LOD for both Au@MIP substrates was found to be $1 \times 10^{-9} \text{ mol dm}^{-3}$, which is two orders of magnitude higher if compared with both LODs for the Au@NIP substrate. The LR of both analytes was 1×10^{-9} – $1 \times 10^{-5} \text{ mol dm}^{-3}$. The selectivity of the pyrene-based Au@MIP sensor investigated from three different aqueous PAH mixtures (pyrene/fluoranthene, pyrene/benzo[a]pyrene, and pyrene/fluoranthene/benzo[a]pyrene) was confirmed (with an LOD of $1 \times 10^{-9} \text{ mol dm}^{-3}$), since SERS signals of fluoranthene and benzo[a]pyrene were not detected. This was ascribed to cavity-size selectivity due to template (pyrene) size. Namely, the pyrene molecule (9.013 Å) is smaller than fluoranthene (9.467 Å) and benzo[a]pyrene (9.820 Å). Concerning the same experiments with fluoranthene-based Au@MIPs substrate, the presence of both fluoranthene and pyrene was confirmed, suggesting that cavity-size selectivity depends on the molecular dimension. Pyrene molecules can easily fill the cavity of the fluoranthene-based substrate since it is a smaller molecule than fluoranthene, but vice versa is not possible. This all implies that the selectivity of the Au@MIPs substrate for PAH detection can be altered by an appropriate choice of template molecules. The practical applicability of the Au@MIPs sensor was demonstrated by spiking two real matrices, creek water and seawater, with pyrene. Results have demonstrated that the pyrene-based Au@MIPs-SERS sensor can be used in pyrene detection in real samples without affecting its sensitivity by matrix effect.

Several SERS-based (non-MIP) nanomaterials have been developed for PAH detection. Yu et al. have modified AuNPs with 4-mercaptophenylboronic acid (4-MPBA) conjugated to β -cyclodextrin (β -CD) [209]. The LODs for pyrene and anthracene were $4 \times 10^{-10} \text{ mol dm}^{-3}$ and $4.4 \times 10^{-9} \text{ mol dm}^{-3}$, respectively. The Au@4-MPBA@ β -CD NPs substrate has a lower LOD for pyrene if compared with the MIP-based plasmonic sensor described above. The method was also tested on two analytes in soil sample extracts; the reliability of the method was confirmed by the good recovery rates (101.8% and 102.5% for pyrene and 106.4% and 101.7% for anthracene). The characteristics of this sensor are comparable to the MIP-based SERS sensor in terms of the LOD for pyrene.

Huang et al. designed a nanocomposite SERS-based magnetic Fe₃O₄/Cu₂O-AgNCs sensor [210]. A linear relationship versus the logarithm of the concentrations of PAHs was found between $1 \times 10^{-11} \text{ mol dm}^{-3}$ and $1 \times 10^{-4} \text{ mol dm}^{-3}$. The LODs for naphthalene, benzo(a)pyrene, pyrene, and anthracene were found to be as low as $1 \times 10^{-9} \text{ mol dm}^{-3}$ for the first three PAHs and $1 \times 10^{-10} \text{ mol dm}^{-3}$ for the last one. Sensitive SERS detection of PAHs in actual soil samples was evidenced. The LOD for pyrene was shown to be the same as for the MIP-based SERS sensor, but the LR is wider.

Cappaci et al. developed a SERS-based sensor composed of an Ag nanoparticle overlayer deposited on the Cr/Ag bilayer [211]. This bilayer improved the adhesion of the overlying Ag layer. Finally, Ag/AgCrNPs substrate was treated with inductively coupled plasma in order to induce the formation of SERS-active Ag nanostructures, giving a highly porous 3D-SERS substrate structure. Effective sensing of pyrene with an LOD of $2.3 \times 10^{-8} \text{ mol dm}^{-3}$ was obtained. It appears that the coral-like substrates do not need any further modifications. Throughout this procedure, a functionalization of SERS-active metal surfaces (increase the binding of PAH molecules) was avoided. Although these results are good, in comparison to the MIP-based SERS sensor, the LOD was not so low.

The apparent lack of literature data regarding plasmonic MIP-SERS sensors for PAHs determination can be explained by the fact that SERS-based employment of MIP substrate is a time-consuming procedure if compared to other SERS-based substrates. However, one of the great advantages of these sensors could be found in their selectivity, reusability, and repeatability. An increased number of research papers and the development of novel plasmonic MIP-SERS sensors for PAHs determination can be expected soon, since there is great potential in this field of research.

3.7. Dyes

The worldwide spread of the textile industry is so huge that it generates about 1 trillion dollars annually, representing 7% of world exports [212]. It is targeted as one of the major environment-polluting sectors. The wastewaters produced in textile processing are highly colored and contain complex concentrations of chemicals (dye, detergents, peroxides, and heavy metals). Textile dyes extensively impact the quality of water bodies. Once released into the environment, mainly water, textile dyes prevent light penetration through water, reducing photosynthesis and dissolved oxygen and distressing the entire aquatic biota [213]. They increase biochemical and chemical oxygen demand, harm photosynthesis, and reduce plant growth. The dyes are soluble organic compounds [212,214], making them easy to spread in the environment. By entering the food chain, they are causing toxicity, mutagenicity, and carcinogenicity. Exposure to textile dyes can lead to many diseases, from dermatitis to central nervous system disorders [212,215]. They are also related to the substitution of enzymatic cofactors, resulting in the inactivation of the enzymatic activities [212,216]. The acute toxicity to textile dyes is mainly caused by oral ingestion and inhalation [212,217], leading to skin and eye irritations [212,218]. Long-term hazard to human health is reflected in the genotoxicity of textile dyes [212,219] and their mutagenic potential [212,220]. Despite the awareness of their toxicity, many carcinogenic dyes are still available on the market [212,221].

Most of the conventional analytical methods used for the detection of organic dyes include high-performance liquid chromatography (HPLC), Ultra-high-performance liquid chromatography-MS/MS (UPLC-MS/MS), and spectrophotometry as instrumental techniques, giving highly accurate results [222–224].

As mentioned, these methods often comprise expensive instrumentation and materials, leading to rather complicated procedures requiring a large volume of solvents and generating large amounts of waste. It consequently implies that these methods are time-consuming, restraining their extensive applications. Therefore, the set-up of a novel, cost-effective, elegant, and rapid alternative technique for accurately detecting organic dyes is a great challenge.

MIP plasmonic sensors are found to be efficient, selective, rapid, and cost-effective alternatives for the detection of organic dyes. The MIP plasmonic sensors used for dye detection and their characteristics are presented in Table 7.

Table 7. MIP plasmonic sensors for dye detection.

Analyte	Functional Monomer	Sensor Type	Linearity Range [mol dm ⁻³]	Limit of Detection [mol dm ⁻³]	Reference
Orange II	AM	SERS	(1–100) × 10 ⁻¹⁰	1 × 10 ⁻¹⁰	[225]
Rhodamine B	AM	SERS	5 × 10 ⁻¹¹ –1 × 10 ⁻⁶	5 × 10 ⁻¹¹	[226]
Rhodamine 6G	AM	SERS	1 × 10 ⁻¹² –1 × 10 ⁻⁶	1 × 10 ⁻¹²	[227]
Rhodamine 6G	AM	SERS	1 × 10 ⁻¹² –1 × 10 ⁻⁷	1 × 10 ⁻¹²	[228]
Sudan I	MAA	SPR	(2–16) × 10 ⁻⁷	1.2 × 10 ⁻⁷	[229]

AM—acrylamide; MAA—methacrylic acid.

As can be seen from Table 7, there are only five MIP-based plasmonic sensors available for textile dye detection. AM and MAA are functional monomers used for MIP synthesis. Methods used for the detection are SPR and SERS. Combining the SERS technique and MIP technology provides sensors for the detection of organic dyes with desirable low LODs (1 × 10⁻¹²–1 × 10⁻⁶ mol dm⁻³), high selectivity and reproducibility, and the capability of replacing conventional methods. Some comprehensive studies regarding accomplished achievements in the field of MIP plasmonic sensors for dye detection, such as this, can provide novel perspectives for finding a suitable choice for their production on an industrial scale.

Xue et al. developed an MIP-SERS sensor with a substrate composed of a metal-organic framework (MOF), UIO-66, modified with polydopamine and silver nanoparticles [225] (Table 7). The substrate was synthesized in the presence of Orange II (OII). Besides the MIP-based sensor, an NIP sensor was synthesized by the same approach but without adding template molecules. The positive effect of MIP technology on the SERS detection ability of materials was confirmed by a comparative analysis of the mentioned sensors. Without specific recognition sites, the NIP sensor showed poor detection sensitivity at low concentrations of organic dyes such as OII. The stability of this sensor for 45 days was confirmed, as well as repeatability and reusability. Concerning selectivity, two dyes, methyl orange and Rhodamine B, were investigated as the competitive (interfering) molecules. The characteristic peak intensity of OII (target molecule) was more than five times higher than the interfering molecules. Chemical composition and three-dimensional structure prevent interfering molecules from passing through the imprinting layer by the so-called “gate effect” and achieving more contact with active sites inside. This sensor has shown recovery values ranging from 92.2% to 114.4% for spiked lake water samples with OII (1 × 10⁻¹⁰–1 × 10⁻⁴ mol dm⁻³). The application of MOF as a part of the MIP-SERS sensor has been further investigated by Li et al. [226]. The investigated imprinted sensor is composed of MOF, a liquid metal core within a zeolitic imidazolate framework shell, Ag NPs, and Rhodamine B dye (RhB). The analog non-MIP sensor was synthesized by a similar procedure, lacking template molecules addition. The LOD for the non-MIP-based sensor was 1 × 10⁻⁸ mol dm⁻³, which is considerably higher than the MIP variant (1 × 10⁻¹¹ mol dm⁻³). The stability test showed a storage time of 60 days. Methyl orange and methylene blue were chosen as the competitive molecules. The resulting intensity of the characteristic peak of RhB was more than three times higher than the peak of interfering molecules. This specific recognition capability is achieved by the “gate effect”. The recovery values for the investigated MIP sensor for spiked river water samples with RhB ranged between 95.9% and 105.7%. All the presented results imply that SERS and MOF-based MIP sensors could be considered a promising combination with advanced characteristics for detecting OII and other residual dyes in the environment. Further investigation of using MOFs as a constituent of SERS-based MIP sensors can be particularly important.

For Rhodamine 6G dye (R6G), there are two MIP-based plasmonic sensors in the literature. Li et al. introduced a novel sensor labeled SiO₂/Ag/MIPs-SERS. The MIP substrate was prepared by precipitation polymerization with SiO₂/Ag nanocomposite particles and R6G [227]. Non-imprinted substrate SiO₂/Ag/NIP, without the R6G, was prepared for a comparison test. The NIP sensor showed an LOD of 1 × 10⁻⁸ mol dm⁻³,

much higher than the LOD of the MIP analog (1×10^{-12} mol dm⁻³). The sensor's selectivity was checked by introducing two dyes, RhB and crystal violet, as the competitive molecules. Obtained results show modest selectivity of the investigated MIP [225]. It can be ascribed to the fact that R6B and RB molecules have a similar structure. In addition, both RhB and crystal violet molecules are smaller than R6B. Another SERS-based MIP sensor for the detection of organic dyes using R6G as a template molecule was developed by Le et al. [228]. The substrate consists of ZnO/Ag heterostructures prepared via a sol-gel method from the AgNPs arranged on the surface of ZnO nanorods (NRs) modified with γ -methacryloxypropyltrimethoxysilane (MPS). The selectivity of this sensor was checked by introducing two dyes, RhB and crystal violet, as the competitive molecules. The Raman signals of the three compounds adsorbed on the sensor substrate were discreet, indicating hardly any specific recognition sites formed. A repeatability test revealed that the SERS intensity weakened by approximately 15% after the fifth cyclic experiment, showing that the investigated sensor possessed self-cleaning and reproducibility properties.

Xu et al. fabricated SRP-based MIP and non-MIP sensors with Au for the detection of Sudan dyes, where Sudan I dye was used as a template molecule [229]. A fast response time of 400 s can be highlighted as one of the advantages of this sensor. Regarding the issue of selectivity, the MIP variant of the sensor can identify Sudan I clearly but is also structurally associated with Sudan II-IV dyes. On the other hand, the non-MIP variant provided an inadequate response for all dyes. It all confirmed the importance of the application of MIP technology to achieve selectivity.

There are many other types of sensors for dye detection. Plasmonic graphene oxide-silver nanocomposite (GO-Ag NPS) substrate for SERS detection of dyes was tested on crystal violet, malachite green, methylene blue, and R6G [230]. The LOD values for all dyes were proximately 1×10^{-6} mol dm⁻³, which is far higher than for MIP-SERS sensors presented in Table 7. In addition, Byram et al. fabricated sensors using Ag nanoparticles and nanostructures as SERS-based platforms through laser ablation in liquids. The sensor allowed sensitive and selective detection of several dyes: R6G, methylene blue, crystal violet, and malachite green. The LOD was found in the nanomolar range, which is 10 to 1000 higher if compared with MIP-SERS sensors presented in Table 7. Moreover, Adade et al. developed a SERS-based sensor to detect Sudan II and IV dyes [231]. The substrate was obtained by galvanic substitution using silver nanoparticles. The obtained LODs for Sudan II (1×10^{-11} mol dm⁻³) and Sudan IV (5×10^{-12} mol dm⁻³) are comparable with MIP-SERS sensors presented in Table 7.

4. Concluding Remarks and Future Perspective

Detecting and monitoring environmental contaminants is an inevitable challenge in different research fields. The increasing waste fabrication and new product development constantly introduce well-known and unknown pollutants into the environment. Therefore, it requires constant development and improvement of analytical sensors for tracking environmental contaminants.

The MIP plasmonic-based sensors discussed in this paper highlight the need for strategies to enhance selectivity due to the high complexity of the environmental matrixes. The demand for high sample throughput analysis must focus on developing selective sensors to avoid time-consuming sample preparation steps and separation techniques, such as different types of chromatography. Besides providing selectivity, MIPs are robust, stable in aqueous and organic solvents, stable at extreme pHs and temperatures, and include a low-cost synthesis procedure. Therefore, they are great candidates to gain more applications in the field of environmental protection, especially in combination with plasmonic-based techniques. Plasmonic-based sensors hold huge potential for environmental contaminants detection. General advantages include rapid sampling, a lower LOD, a broad LR, high sensitivity, and high selectivity. Specific sensing based on plasmonic platforms (SPR, LSPR, SEF, SERS, and SEIRA) is a good choice for different applications.

Recent years have witnessed the successful development and wide applications of MIP plasmonic-based sensors. Still, some challenges need to be addressed. Critical aspects are improving the sensitivity, enhancing reproducibility, and expanding the application of MIP plasmonic-based sensors. Sensitivity is a crucial parameter to evaluate the performance of any sensor. Various approaches are used to overcome this issue in different plasmonic-based sensors. For example, improving the sensitivity of MIP-SERS sensors can be accomplished by preparing novel SERS substrates or using controllable aggregation detection modes. On the other hand, the performance improvement of fiber SPR sensors can be achieved by heightening the overlap integral of the surface plasmon polaritons' electric field intensity on the sensor surface. Reproducibility is also vital to establish the practical application performances of the sensor. In MIP SERS-based sensors, it is closely related to the reproducibility of the SERS substrates and can be improved by introducing internal standards or by preparing highly uniform SERS substrates.

To date, research on MIP plasmonic-based sensors is mainly at the stage of structural design and proof-of-concept detection in the lab. The practical applications are far from possible at the moment. With the development of MIP plasmonic-based sensors, the application research should be motivated. Considering the advantages of MIP plasmonic-based sensors, such as miniaturization, rapidity, high selectivity, and sensitivity, successful applications in many fields can be expected.

For now, MIP plasmonic-based sensors have mainly found their application in the biomedical field. In the area of environmental protection, there are not a great number of constructed sensors relying on these technologies at this moment. Despite the promise of rapid detection, the technology requires certain developments in order to transfer from lab to field applications. Additional efforts must be devoted to overcoming some limitations of MIPs in order to increase their mass production potentials, such as heterogeneous particle size, irregular shape, and unspecific binding sites. It will consequently expand the development of new sensors, especially applied to environmental analysis. Regarding plasmonic-based sensing, there are also some limitations. Factors that should be taken into account are cost, user interface, robustness, and connectivity, which would allow online monitoring. With exponential technology growth, science will unquestionably provide these answers soon, making MIP plasmonic-based sensors a realistic prospect for environmental health and protection in the near future.

Author Contributions: Conceptualization, T.L.-P.; investigation, T.L.-P., T.T., V.M. and N.P.; writing—original draft preparation, T.L.-P., T.T., V.M. and N.P.; writing—review and editing, T.L.-P., T.T., V.M. and N.P.; supervision, T.L.-P.; funding acquisition, T.L.-P. All authors have read and agreed to the published version of the manuscript.

Funding: The authors acknowledge the support provided by the Serbian Ministry of Education, Science and Technological Development (Contract number: 451-03-68/2022-14/200017).

Institutional Review Board Statement: Not applicable.

Informed Consent Statement: Not applicable.

Data Availability Statement: Not applicable.

Conflicts of Interest: The authors declare no conflict of interest.

References

1. Avio, C.G.; Gorbi, S.; Regoli, F. Plastics and microplastics in the oceans: From emerging pollutants to emerged threat. *Mar. Environ. Res.* **2017**, *128*, 2–11. [[CrossRef](#)] [[PubMed](#)]
2. Calvo-Flores, F.G.; Isac-García, J.; Dobado, J.A. *Emerging Pollutants: Origin, Structure, and Properties*; John Wiley & Sons: Hoboken, NJ, USA, 2018.
3. Tang, Y.; Yin, M.; Yang, W.; Li, H.; Zhong, Y.; Mo, L.; Liang, Y.; Ma, X.; Sun, X. Emerging pollutants in water environment: Occurrence, monitoring, fate, and risk assessment. *Water Environ. Res.* **2019**, *91*, 984–991. [[CrossRef](#)] [[PubMed](#)]
4. Kumar, M.; Borah, P.; Devi, P. Chapter 3—Priority and emerging pollutants in water. In *Inorganic Pollutants in Water*; Devi, P., Singh, P., Kansal, S.K., Eds.; Elsevier: Amsterdam, The Netherlands, 2020; pp. 33–49.

5. Keitel, B.; Batista, A.D.; Mizaikoff, B.; Fresco-Cala, B. Molecularly Imprinted Polymer Sensors in Environmental Analysis. *Encycl. Sens. Biosens.* **2022**, *4*, 851–867. [[CrossRef](#)]
6. Benotti, M.J.; Trenholm, R.A.; Vanderford, B.J.; Holady, J.C.; Stanford, B.D.; Snyder, S. Pharmaceuticals and Endocrine Disrupting Compounds in U.S. Drinking Water. *Environ. Sci. Technol.* **2008**, *43*, 597–603. [[CrossRef](#)] [[PubMed](#)]
7. Wilkinson, J.L.; Boxall, A.B.; Kolpin, D.W.; Leung, K.M.; Lai, R.W.; Galbán-Malagón, C.; Adell, A.D.; Mondon, J.; Metian, M.; Marchant, R.A. Pharmaceutical pollution of the world's rivers. *Proc. Natl. Acad. Sci. USA* **2022**, *119*, e2113947119. [[CrossRef](#)]
8. Andres, L.; Boateng, K.; Borja-Vega, C.; Thomas, E. A Review of In-Situ and Remote Sensing Technologies to Monitor Water and Sanitation Interventions. *Water* **2018**, *10*, 756. [[CrossRef](#)]
9. Huang, Y.; Wang, T.; Xu, Z.; Hughes, E.; Qian, F.; Lee, M.; Fan, Y.; Lei, Y.; Brückner, C.; Li, B. Real-Time in Situ Monitoring of Nitrogen Dynamics in Wastewater Treatment Processes using Wireless, Solid-State, and Ion-Selective Membrane Sensors. *Environ. Sci. Technol.* **2019**, *53*, 3140–3148. [[CrossRef](#)]
10. Pejčić, B.; Myers, M.; Ross, A. Mid-Infrared Sensing of Organic Pollutants in Aqueous Environments. *Sensors* **2009**, *9*, 6232–6253. [[CrossRef](#)]
11. Zhu, Z.; Su, Y.; Li, J.; Li, D.; Zhang, J.; Song, S.; Zhao, Y.; Li, G.; Fan, C. Highly Sensitive Electrochemical Sensor for Mercury(II) Ions by Using a Mercury-Specific Oligonucleotide Probe and Gold Nanoparticle-Based Amplification. *Anal. Chem.* **2009**, *81*, 7660–7666. [[CrossRef](#)]
12. Yan, X.; Li, H.; Su, X. Review of optical sensors for pesticides. *TrAC Trends Anal. Chem.* **2018**, *103*, 1–20. [[CrossRef](#)]
13. Saleh, T.A.; Fadillah, G.; Saputra, O.A. Nanoparticles as components of electrochemical sensing platforms for the detection of petroleum pollutants: A review. *TrAC Trends Anal. Chem.* **2019**, *118*, 194–206. [[CrossRef](#)]
14. Patel, B.R.; Noroozifar, M.; Kerman, K. Review—Nanocomposite-Based Sensors for Voltammetric Detection of Hazardous Phenolic Pollutants in Water. *J. Electrochem. Soc.* **2020**, *167*, 037568. [[CrossRef](#)]
15. Fresco-Cala, B.; Mizaikoff, B. Surrogate Imprinting Strategies: Molecular Imprints via Fragments and Dummies. *ACS Appl. Polym. Mater.* **2020**, *2*, 3714–3741. [[CrossRef](#)]
16. Fresco-Cala, B.; Batista, A.; Cárdenas, S. Molecularly Imprinted Polymer Micro- and Nano-Particles: A Review. *Molecules* **2020**, *25*, 4740. [[CrossRef](#)]
17. Piletsky, S.; Canfarotta, F.; Poma, A.; Bossi, A.M.; Piletsky, S. Molecularly Imprinted Polymers for Cell Recognition. *Trends Biotechnol.* **2019**, *38*, 368–387. [[CrossRef](#)]
18. Armutcu, C.; Özgür, E.; Çorman, M.E.; Uzun, L. Interface imprinted polymers with well-oriented recognition sites for selective purification of hemoglobin. *Colloids Surf. B Biointerfaces* **2020**, *197*, 111435. [[CrossRef](#)]
19. Chiappini, A.; Pasquardini, L.; Bossi, A.M. Molecular Imprinted Polymers Coupled to Photonic Structures in Biosensors: The State of Art. *Sensors* **2020**, *20*, 5069. [[CrossRef](#)]
20. Ozelikay, G.; Kaya, S.; Ozkan, E.; Cetinkaya, A.; Nemitlu, E.; Kır, S.; Ozkan, S. Sensor-based MIP technologies for targeted metabolomics analysis. *TrAC Trends Anal. Chem.* **2021**, *146*, 116487. [[CrossRef](#)]
21. Bigdeli, A.; Ghasemi, F.; Golmohammadi, H.; Abbasi-Moayed, S.; Nejad, M.A.F.; Fahimi-Kashani, N.; Jafarinejad, S.; Shahrajabian, M.; Hormozi-Nezhad, M.R. Nanoparticle-based optical sensor arrays. *Nanoscale* **2017**, *9*, 16546–16563. [[CrossRef](#)]
22. Fauzi, N.; Fen, Y.; Omar, N.; Hashim, H. Recent Advances on Detection of Insecticides Using Optical Sensors. *Sensors* **2021**, *21*, 3856. [[CrossRef](#)]
23. Farre, M.; Martinez, E.; Barcelu, D.; Yolanda, P. *Sensor, Biosensors and MIP Based Sensors in Food Toxicants Analysis*; Elsevier: Amsterdam, The Netherlands, 2007.
24. Roda, A.; Michelini, E.; Cevenini, L.; Calabria, D.; Calabretta, M.M.; Simoni, P. Integrating Biochemiluminescence Detection on Smartphones: Mobile Chemistry Platform for Point-of-Need Analysis. *Anal. Chem.* **2014**, *86*, 7299–7304. [[CrossRef](#)] [[PubMed](#)]
25. Tütüncü, E.; Kokoric, V.; Wilk, A.; Seichter, F.; Schmid, M.; Hunt, W.E.; Manuel, A.M.; Mirkarimi, P.; Alameda, J.B.; Carter, J.C.; et al. Fiber-Coupled Substrate-Integrated Hollow Waveguides: An Innovative Approach to Mid-infrared Remote Gas Sensors. *ACS Sens.* **2017**, *2*, 1287–1293. [[CrossRef](#)] [[PubMed](#)]
26. Soares, S.; Rosado, T.; Barroso, M.; Vieira, D.N.; Gallardo, E. Organophosphorus pesticide determination in biological specimens: Bioanalytical and toxicological aspects. *Int. J. Leg. Med.* **2019**, *133*, 1763–1784. [[CrossRef](#)] [[PubMed](#)]
27. Leung, M.C.; Meyer, J.N. Mitochondria as a target of organophosphate and carbamate pesticides: Revisiting common mechanisms of action with new approach methodologies. *Reprod. Toxicol.* **2019**, *89*, 83–92. [[CrossRef](#)] [[PubMed](#)]
28. Helmerhorst, E.; Chandler, D.J.; Nussio, M.; Mamotte, C.D. Real-time and Label-free Bio-sensing of Molecular Interactions by Surface Plasmon Resonance: A Laboratory Medicine Perspective. *Clin. Biochem. Rev.* **2012**, *33*, 161–173.
29. Shrivastav, A.M.; Cvelbar, U.; Abdulhalim, I. A comprehensive review on plasmonic-based biosensors used in viral diagnostics. *Commun. Biol.* **2021**, *4*, 70. [[CrossRef](#)]
30. Kretschmann, E.; Raether, H. Notizen: Radiative Decay of Non Radiative Surface Plasmons Excited by Light. *Z. Nat. A* **1968**, *23*, 2135–2136. [[CrossRef](#)]
31. Sharma, A.K.; Jha, R.; Gupta, B.D. Fiber-Optic Sensors Based on Surface Plasmon Resonance: A Comprehensive Review. *IEEE Sens. J.* **2007**, *7*, 1118–1129. [[CrossRef](#)]
32. Mayer, K.M.; Hafner, J.H. Localized surface plasmon resonance sensors. *Chem. Rev.* **2011**, *111*, 3828–3857. [[CrossRef](#)]
33. Li, J.-F.; Li, C.-Y.; Aroca, R.F. Plasmon-enhanced fluorescence spectroscopy. *Chem. Soc. Rev.* **2017**, *46*, 3962–3979. [[CrossRef](#)]

34. Li, P.; Long, F.; Chen, W.; Chen, J.; Chu, P.K.; Wang, H. Fundamentals and applications of surface-enhanced Raman spectroscopy-based biosensors. *Curr. Opin. Biomed. Eng.* **2019**, *13*, 51–59. [CrossRef]
35. Ataka, K.; Heberle, J. Biochemical applications of surface-enhanced infrared absorption spectroscopy. *Anal. Bioanal. Chem.* **2007**, *388*, 47–54. [CrossRef]
36. Alavanja, M.C.R.; Bonner, M.R. Occupational Pesticide Exposures and Cancer Risk: A Review. *J. Toxicol. Environ. Health Part B* **2012**, *15*, 238–263. [CrossRef]
37. Lazarevic-Pasti, T.; Leskovac, A.; Vasic, V. Myeloperoxidase Inhibitors as Potential Drugs. *Curr. Drug Metab.* **2015**, *16*, 168–190. [CrossRef]
38. Lazarevic-Pasti, T.; Leskovac, A.; Momic, T.; Petrovic, S.; Vasic, V. Modulators of acetylcholinesterase activity: From Alzheimer's disease to anti-cancer drugs. *Curr. Med. Chem.* **2017**, *24*, 3283–3309. [CrossRef]
39. Gilboa-Geffen, A.; Hartmann, G.; Soreq, H. Stressing hematopoiesis and immunity: An acetylcholinesterase window into nervous and immune system interactions. *Front. Mol. Neurosci.* **2012**, *5*, 30. [CrossRef]
40. Hernández, A.F.; Menéndez, P. Linking Pesticide Exposure with Pediatric Leukemia: Potential Underlying Mechanisms. *Int. J. Mol. Sci.* **2016**, *17*, 461. [CrossRef]
41. National Collaborating Centre for Mental Health (UK). Depression in Adults with a Chronic Physical Health Problem: Treatment and Management. NICE Clinical Guidelines, No. 91. British Psychological Society (UK). 2010. Available online: <https://www.ncbi.nlm.nih.gov/books/NBK82916/> (accessed on 30 November 2022).
42. Anicijevic, V.; Lazarević-Pašti, T. *Organophosphates—Application, Effects on Human Health and Removal*; Nova Science Publishers: New York, NY, USA, 2020; pp. 1–42.
43. Sanne, B.; Mykletun, A.; Dahl, A.A.; Moen, B.E.; Tell, G.S. Occupational Differences in Levels of Anxiety and Depression: The Hordaland Health Study. *J. Occup. Environ. Med.* **2003**, *45*, 628–638. [CrossRef]
44. Harrison, V.; Mackenzie Ross, S. Anxiety and depression following cumulative low-level exposure to organophosphate pesticides. *Environ. Res.* **2016**, *151*, 528–536. [CrossRef]
45. World Health Organization. *International Programme on Chemical Safety. The WHO Recommended Classification of Pesticides by Hazard and Guidelines to Classification 2009*; World Health Organization: Geneva, Switzerland, 2010.
46. Cakir, O.; Bakhshpour, M.; Yilmaz, F.; Baysal, Z. Novel QCM and SPR sensors based on molecular imprinting for highly sensitive and selective detection of 2,4-dichlorophenoxyacetic acid in apple samples. *Mater. Sci. Eng. C* **2019**, *102*, 483–491. [CrossRef]
47. Çakır, O.; Bakhshpour, M.; Göktürk, I.; Yilmaz, F.; Baysal, Z. Sensitive and selective detection of amitrole based on molecularly imprinted nanosensor. *J. Mol. Recognit.* **2021**, *34*, e2929. [CrossRef] [PubMed]
48. Zhao, N.; Chen, C.; Zhou, J. Surface plasmon resonance detection of ametryn using a molecularly imprinted sensing film prepared by surface-initiated atom transfer radical polymerization. *Sens. Actuators B Chem.* **2012**, *166–167*, 473–479. [CrossRef]
49. Wei, C.; Zhou, H.; Zhou, J. Ultrasensitively sensing acephate using molecular imprinting techniques on a surface plasmon resonance sensor. *Talanta* **2011**, *83*, 1422–1427. [CrossRef] [PubMed]
50. Agrawal, H.; Shrivastav, A.; Gupta, B.D. Surface plasmon resonance based optical fiber sensor for atrazine detection using molecular imprinting technique. *Sens. Actuators B Chem.* **2015**, *227*, 204–211. [CrossRef]
51. Zhao, B.; Feng, S.; Hu, Y.; Wang, S.; Lu, X. Rapid determination of atrazine in apple juice using molecularly imprinted polymers coupled with gold nanoparticles-colorimetric/SERS dual chemosensor. *Food Chem.* **2018**, *276*, 366–375. [CrossRef]
52. Saylan, Y.; Akgönüllü, S.; Çimen, D.; Derazshamshir, A.; Bereli, N.; Yilmaz, F.; Denizli, A. Development of surface plasmon resonance sensors based on molecularly imprinted nanofilms for sensitive and selective detection of pesticides. *Sensors Actuators B Chem.* **2017**, *241*, 446–454. [CrossRef]
53. Çakır, O.; Bakhshpour, M.; Yilmaz, F.; Baysal, Z. Preparation of Nanoparticle-Amplified Surface Plasmon Resonance Sensors Based on Molecular Imprinting for Pesticide Determination. *J. Inst. Sci. Technol.* **2018**, *8*, 219–226. [CrossRef]
54. Yao, G.-H.; Liang, R.-P.; Huang, C.-F.; Wang, Y.; Qiu, J.-D. Surface Plasmon Resonance Sensor Based on Magnetic Molecularly Imprinted Polymers Amplification for Pesticide Recognition. *Anal. Chem.* **2013**, *85*, 11944–11951. [CrossRef]
55. Feng, S.; Hu, Y.; Ma, L.; Lu, X. Development of molecularly imprinted polymers-surface-enhanced Raman spectroscopy/colorimetric dual sensor for determination of chlorpyrifos in apple juice. *Sens. Actuators B Chem.* **2017**, *241*, 750–757. [CrossRef]
56. Cheshari, E.C.; Ren, X.; Li, X. Core-shell Ag-molecularly imprinted composite for SERS detection of carbendazim. *Int. J. Environ. Anal. Chem.* **2019**, *100*, 1245–1258. [CrossRef]
57. Çakır, O.; Baysal, Z. Pesticide analysis with molecularly imprinted nanofilms using surface plasmon resonance sensor and LC-MS/MS: Comparative study for environmental water samples. *Sens. Actuators B Chem.* **2019**, *297*, 126764.
58. Shrivastav, A.M.; Gupta, B.D. Molecularly Imprinted Fiber Optic SPR Sensor for Parathion Methyl Detection. In *Frontiers in Optics 2015*; Optica Publishing Group: San Jose, CA, USA, 2015.
59. Kou, Y.; Wu, T.; Zheng, H.; Kadasala, N.R.; Yang, S.; Guo, C.; Chen, L.; Liu, Y.; Yang, J. Recyclable Magnetic MIP-Based SERS Sensors for Selective, Sensitive, and Reliable Detection of Paclitaxel Residues in Complex Environments. *ACS Sustain. Chem. Eng.* **2020**, *8*, 14549–14556. [CrossRef]
60. Xu, W.; Wang, Q.; Huang, W.; Yang, W. Construction of a novel electrochemical sensor based on molecularly imprinted polymers for the selective determination of chlorpyrifos in real samples. *J. Sep. Sci.* **2017**, *40*, 4839–4846. [CrossRef]

61. Fan, M.; Gan, T.; Yin, G.; Cheng, F.; Zhao, N. Molecularly imprinted polymer coated Mn-doped ZnS quantum dots embedded in a metal–organic framework as a probe for selective room temperature phosphorescence detection of chlorpyrifos. *RSC Adv.* **2021**, *11*, 27845–27854. [[CrossRef](#)]
62. Xie, C.; Li, H.; Li, S.; Gao, S. Surface molecular imprinting for chemiluminescence detection of the organophosphate pesticide chlorpyrifos. *Microchim. Acta* **2011**, *174*, 311–320. [[CrossRef](#)]
63. Wang, Y.; Cui, Z.; Zhang, X.; Zhang, X.; Zhu, Y.; Chen, S.; Hu, H. Excitation of Surface Plasmon Resonance on Multiwalled Carbon Nanotube Metasurfaces for Pesticide Sensors. *ACS Appl. Mater. Interfaces* **2020**, *12*, 52082–52088. [[CrossRef](#)]
64. Li, Q.; Dou, X.; Zhang, L.; Zhao, X.; Luo, J.; Yang, M. Oriented assembly of surface plasmon resonance biosensor through staphylococcal protein A for the chlorpyrifos detection. *Anal. Bioanal. Chem.* **2019**, *411*, 6057–6066. [[CrossRef](#)]
65. Xu, Q.; Guo, X.; Xu, L.; Ying, Y.; Wu, Y.; Wen, Y.; Yang, H. Template-free synthesis of SERS-active gold nanopopcorn for rapid detection of chlorpyrifos residues. *Sens. Actuators B Chem.* **2017**, *241*, 1008–1013. [[CrossRef](#)]
66. Thepudom, T.; Lertvachirapaiboon, C.; Shinbo, K.; Kato, K.; Kaneko, F.; Kerdcharoen, T.; Baba, A. Surface plasmon resonance-enhanced photoelectrochemical sensor for detection of an organophosphate pesticide chlorpyrifos. *MRS Commun.* **2018**, *8*, 107–112. [[CrossRef](#)]
67. Soongsong, J.; Lerdsri, J.; Jakmunee, J. A facile colorimetric aptasensor for low-cost chlorpyrifos detection utilizing gold nanoparticle aggregation induced by polyethyleneimine. *Analyst* **2021**, *146*, 4848–4857. [[CrossRef](#)]
68. Zhang, H.; Qu, Y.; Zhang, Y.; Yan, Y.; Gao, H. Thioglycolic acid-modified AuNPs as a colorimetric sensor for the rapid determination of the pesticide chlorpyrifos. *Anal. Methods* **2022**, *14*, 1996–2002. [[CrossRef](#)] [[PubMed](#)]
69. Guler, M.; Turkoglu, V.; Basi, Z. Determination of malation, methidathion, and chlorpyrifos ethyl pesticides using acetylcholinesterase biosensor based on Nafion/Ag@rGO-NH₂ nanocomposites. *Electrochim. Acta* **2017**, *240*, 129–135. [[CrossRef](#)]
70. Liu, Q.; He, Z.; Wang, H.; Feng, X.; Han, P. Magnetically controlled colorimetric aptasensor for chlorpyrifos based on copper-based metal-organic framework nanoparticles with peroxidase mimetic property. *Mikrochim. Acta* **2020**, *187*, 524. [[CrossRef](#)] [[PubMed](#)]
71. Saranya, S.; Deepa, P. Perforated oxidized graphitic carbon nitride with Nickel spikes as efficient material for electrochemical sensing of chlorpyrifos in water samples. *Surf. Interfaces* **2022**, *32*, 102170. [[CrossRef](#)]
72. Salahshoor, Z.; Ho, K.-V.; Hsu, S.-Y.; Lin, C.-H.; de Cortalezzi, M.F. Detection of Atrazine and its metabolites by photonic molecularly imprinted polymers in aqueous solutions. *Chem. Eng. J. Adv.* **2022**, *12*, 100368. [[CrossRef](#)]
73. Chen, Q.; Lu, H.; Zhang, Z.; Du, B.; Liu, M.; Zhao, G. Visible-light-driven molecularly imprinted self-powered sensor for atrazine with high sensitivity and selectivity by separating photoanode from recognition element. *Sens. Actuators B Chem.* **2022**, *360*, 131670. [[CrossRef](#)]
74. Yola, M.L.; Atar, N. Electrochemical Detection of Atrazine by Platinum Nanoparticles/Carbon Nitride Nanotubes with Molecularly Imprinted Polymer. *Ind. Eng. Chem. Res.* **2017**, *56*, 7631–7639. [[CrossRef](#)]
75. Nsiband, S.A.; Forbes, P.B. Development of a quantum dot molecularly imprinted polymer sensor for fluorescence detection of atrazine. *Luminescence* **2019**, *34*, 480–488. [[CrossRef](#)]
76. Eskandari, V.; Kordzadeh, A.; Zeinalizad, L.; Sahbafar, H.; Aghanouri, H.; Hadi, A.; Ghaderi, S. Detection of molecular vibrations of atrazine by accumulation of silver nanoparticles on flexible glass fiber as a surface-enhanced Raman plasmonic nanosensor. *Opt. Mater.* **2022**, *128*, 112310. [[CrossRef](#)]
77. Albarghouthi, N.; MacMillan, P.; Brosseau, C.L. Optimization of gold nanorod arrays for surface enhanced Raman spectroscopy (SERS) detection of atrazine. *Analyst* **2021**, *146*, 2037–2047. [[CrossRef](#)]
78. Tang, J.; Chen, W.; Ju, H. Sensitive surface-enhanced Raman scattering detection of atrazine based on aggregation of silver nanoparticles modified carbon dots. *Talanta* **2019**, *201*, 46–51. [[CrossRef](#)]
79. Daoudi, K.; Gaidi, M.; Columbus, S.; Shameer, M.; Alawadhi, H. Hierarchically assembled silver nanoprism-graphene oxide-silicon nanowire arrays for ultrasensitive surface enhanced Raman spectroscopy sensing of atrazine. *Mater. Sci. Semicond. Process.* **2021**, *138*, 106288. [[CrossRef](#)]
80. Supraja, P.; Tripathy, S.; Vanjari, S.R.K.; Singh, V.; Singh, S.G. Electrospun tin (IV) oxide nanofiber based electrochemical sensor for ultra-sensitive and selective detection of atrazine in water at trace levels. *Biosens. Bioelectron.* **2019**, *141*, 111441. [[CrossRef](#)]
81. Fan, L.; Zhang, C.; Liang, G.; Yan, W.; Guo, Y.; Bi, Y.; Dong, C. Highly sensitive photoelectrochemical aptasensor based on MoS₂ quantum dots/TiO₂ nanotubes for detection of atrazine. *Sens. Actuators B Chem.* **2021**, *334*, 129652. [[CrossRef](#)]
82. Huang, X.; Li, H.; Hu, M.; Bai, M.; Guo, Y.; Sun, X. Effective Electrochemiluminescence Aptasensor for Detection of Atrazine Residue. *Sensors* **2022**, *22*, 3430. [[CrossRef](#)]
83. Liguori, K.; Keenum, I.; Davis, B.C.; Calarco, J.; Milligan, E.; Harwood, V.J.; Pruden, A. Antimicrobial Resistance Monitoring of Water Environments: A Framework for Standardized Methods and Quality Control. *Environ. Sci. Technol.* **2022**, *56*, 9149–9160. [[CrossRef](#)]
84. Rastogi, A.; Tiwari, M.K.; Ghangrekar, M.M. A review on environmental occurrence, toxicity and microbial degradation of Non-Steroidal Anti-Inflammatory Drugs (NSAIDs). *J. Environ. Manag.* **2021**, *300*, 113694. [[CrossRef](#)]
85. Ayankojo, A.G.; Reut, J.; Öpik, A.; Furchner, A.; Syritski, V. Hybrid molecularly imprinted polymer for amoxicillin detection. *Biosens. Bioelectron.* **2018**, *118*, 102–107. [[CrossRef](#)]
86. Yola, M.L.; Eren, T.; Atar, N. Molecular imprinted nanosensor based on surface plasmon resonance: Application to the sensitive determination of amoxicillin. *Sens. Actuators B Chem.* **2014**, *195*, 28–35. [[CrossRef](#)]

87. Bereli, N.; Çimen, D.; Hüseyinli, S.; Denizli, A. Detection of amoxicillin residues in egg extract with a molecularly imprinted polymer on gold microchip using surface plasmon resonance and quartz crystal microbalance methods. *J. Food Sci.* **2020**, *85*, 4152–4160. [[CrossRef](#)]
88. Faalnouri, S.; Çimen, D.; Bereli, N.; Denizli, A. Surface Plasmon Resonance Nanosensors for Detecting Amoxicillin in Milk Samples with Amoxicillin Imprinted Poly (hydroxyethyl methacrylate-N-methacryloyl-(L)-glutamic acid). *ChemistrySelect* **2020**, *5*, 4761–4769. [[CrossRef](#)]
89. Yola, M.L.; Atar, N.; Eren, T. Determination of amikacin in human plasma by molecular imprinted SPR nanosensor. *Sens. Actuators B Chem.* **2014**, *198*, 70–76. [[CrossRef](#)]
90. Sari, E.; Üzek, R.; Duman, M.; Denizli, A. Detection of ciprofloxacin through surface plasmon resonance nanosensor with specific recognition sites. *J. Biomater. Sci. Polym. Ed.* **2018**, *29*, 1302–1318. [[CrossRef](#)] [[PubMed](#)]
91. Zhang, B.; Pang, K.; Sun, Y.; Wang, X. High-performance bimetallic SPR sensor for ciprofloxacin based on molecularly imprinted polymer. *SPIE Nanosci. Eng.* **2018**, *10728*, 92–97. [[CrossRef](#)]
92. Sullivan, M.V.; Henderson, A.; Hand, R.A.; Turner, N.W. A molecularly imprinted polymer nanoparticle-based surface plasmon resonance sensor platform for antibiotic detection in river water and milk. *Anal. Bioanal. Chem.* **2022**, *414*, 3687–3696. [[CrossRef](#)]
93. Carrasco, S.; Benito-Peña, E.; Navarro-Villoslada, F.; Langer, J.; Sanz-Ortiz, M.N.; Reguera, J.; Liz-Marzán, L.M.; Moreno-Bondi, M.C. Multibranching Gold-Mesoporous Silica Nanoparticles Coated with a Molecularly Imprinted Polymer for Label-Free Antibiotic Surface-Enhanced Raman Scattering Analysis. *Chem. Mater.* **2016**, *28*, 7947–7954. [[CrossRef](#)]
94. Wang, W.; Wang, R.; Liao, M.; Kidd, M.T.; Li, Y. Rapid detection of enrofloxacin using a localized surface plasmon resonance sensor based on polydopamine molecular imprinted recognition polymer. *J. Food Meas. Charact.* **2021**, *15*, 3376–3386. [[CrossRef](#)]
95. Sari, E.; Üzek, R.; Duman, M.; Denizli, A. Fabrication of surface plasmon resonance nanosensor for the selective determination of erythromycin via molecular imprinted nanoparticles. *Talanta* **2016**, *150*, 607–614. [[CrossRef](#)]
96. Zhang, L.; Zhu, C.; Chen, C.; Zhu, S.; Zhou, J.; Wang, M.; Shang, P. Determination of kanamycin using a molecularly imprinted SPR sensor. *Food Chem.* **2018**, *266*, 170–174. [[CrossRef](#)]
97. Wang, J.; Li, X.; Zhang, R.; Fu, B.; Chen, M.; Ye, M.; Liu, W.; Xu, J.; Pan, G.; Zhang, H. A molecularly imprinted antibiotic receptor on magnetic nanotubes for the detection and removal of environmental oxytetracycline. *J. Mater. Chem. B* **2022**, *10*, 6777–6783. [[CrossRef](#)]
98. Verma, R.; Gupta, B.D. Optical fiber sensor for the detection of tetracycline using surface plasmon resonance and molecular imprinting. *Analyst* **2013**, *138*, 7254–7263. [[CrossRef](#)]
99. Bakhshpour, M.; Göktürk, I.; Bereli, N.; Yılmaz, F.; Denizli, A. Selective Detection of Penicillin G Antibiotic in Milk by Molecularly Imprinted Polymer-Based Plasmonic SPR Sensor. *Biomimetics* **2021**, *6*, 72. [[CrossRef](#)]
100. Sui, G.; Yang, X.; Li, H.; Li, Y.; Li, L.; Shao, J.; Li, Y.; Wang, J.; Xue, Y.; Zhang, J.; et al. Synthesis of SERS imprinted membrane based on Ag/ESM with different morphologies for selective detection of antibiotics in aqueous sample. *Opt. Mater.* **2021**, *121*, 111581. [[CrossRef](#)]
101. Nawaz, T.; Ahmad, M.; Yu, J.; Wang, S.; Wei, T. A recyclable tetracycline imprinted polymeric SPR sensor: In synergy with itaconic acid and methacrylic acid. *New J. Chem.* **2020**, *45*, 3102–3111. [[CrossRef](#)]
102. Shrivastav, A.M.; Mishra, S.K.; Gupta, B.D. Localized and propagating surface plasmon resonance based fiber optic sensor for the detection of tetracycline using molecular imprinting. *Mater. Res. Express* **2015**, *2*, 035007. [[CrossRef](#)]
103. Altintas, Z. Surface plasmon resonance based sensor for the detection of glycopeptide antibiotics in milk using rationally designed nanoMIPs. *Sci. Rep.* **2018**, *8*, 11222. [[CrossRef](#)]
104. Henderson, A.; Sullivan, M.V.; Hand, R.A.; Turner, N.W. Detection of selective androgen receptor modulators (SARMs) in serum using a molecularly imprinted nanoparticle surface plasmon resonance sensor. *J. Mater. Chem. B* **2022**, *10*, 6792–6799. [[CrossRef](#)]
105. Özgür, E.; Saylan, Y.; Bereli, N.; Türkmen, D.; Denizli, A. Molecularly imprinted polymer integrated plasmonic nanosensor for cocaine detection. *J. Biomater. Sci. Polym. Ed.* **2020**, *31*, 1211–1222. [[CrossRef](#)] [[PubMed](#)]
106. Özkan, A.; Atar, N.; Yola, M.L. Enhanced surface plasmon resonance (SPR) signals based on immobilization of core-shell nanoparticles incorporated boron nitride nanosheets: Development of molecularly imprinted SPR nanosensor for anticancer drug, etoposide. *Biosens. Bioelectron.* **2019**, *130*, 293–298. [[CrossRef](#)]
107. Decorbie, N.; Tijunelyte, I.; Gam-Derouich, S.; Solard, J.; Lamouri, A.; DeCorse, P.; Felidj, N.; Gauchotte-Lindsay, C.; Rinnert, E.; Mangeney, C.; et al. Sensing Polymer/Paracetamol Interaction with an Independent Component Analysis-Based SERS-MIP Nanosensor. *Plasmonics* **2020**, *15*, 1533–1539. [[CrossRef](#)]
108. Liu, Y.; Bao, J.; Zhang, L.; Chao, C.; Guo, J.; Cheng, Y.; Zhu, Y.; Xu, G. Ultrasensitive SERS detection of propranolol based on sandwich nanostructure of molecular imprinting polymers. *Sens. Actuators B Chem.* **2017**, *255*, 110–116. [[CrossRef](#)]
109. Chen, C.; Wang, X.; Zhang, Y.; Li, X.; Gao, H.; Waterhouse, G.I.; Qiao, X.; Xu, Z. A molecularly-imprinted SERS sensor based on a TiO₂@Ag substrate for the selective capture and sensitive detection of tryptamine in foods. *Food Chem.* **2022**, *394*, 133536. [[CrossRef](#)] [[PubMed](#)]
110. Lavine, B.K.; Westover, D.J.; Kaval, N.; Mirjankar, N.; Oxenford, L.; Mwangi, G.K. Swellable molecularly imprinted polyN-(N-propyl)acrylamide particles for detection of emerging organic contaminants using surface plasmon resonance spectroscopy. *Talanta* **2007**, *72*, 1042–1048. [[CrossRef](#)] [[PubMed](#)]

111. Chullasat, K.; Nurerk, P.; Kanatharana, P.; Davis, F.; Bunkoed, O. A facile optosensing protocol based on molecularly imprinted polymer coated on CdTe quantum dots for highly sensitive and selective amoxicillin detection. *Sens. Actuators B Chem.* **2018**, *254*, 255–263. [CrossRef]
112. Li, S.; Ma, X.; Pang, C.; Li, H.; Liu, C.; Xu, Z.; Luo, J.; Yang, Y. Novel molecularly imprinted amoxicillin sensor based on a dual recognition and dual detection strategy. *Anal. Chim. Acta* **2020**, *1127*, 69–78. [CrossRef] [PubMed]
113. Lu, H.; Huang, Y.; Cui, H.; Li, L.; Ding, Y. A molecularly imprinted electrochemical aptasensor based on zinc oxide and co-deposited gold nanoparticles/reduced graphene oxide composite for detection of amoxicillin. *Mikrochim. Acta* **2022**, *189*, 421. [CrossRef]
114. Ali, W.H.; Dheyab, A.B.; Alwan, A.M.; Abber, Z.S. Study the role of mud-like Psi morphologies on the performance of AuNPS SERS sensor for efficient detection of amoxicillin. *AIP Conf. Proc.* **2020**, *2290*, 050061. [CrossRef]
115. Wang, L.; Zhou, G.; Guan, X.-L.; Zhao, L. Rapid preparation of surface-enhanced Raman substrate in microfluidic channel for trace detection of amoxicillin. *Spectrochim. Acta Part A Mol. Biomol. Spectrosc.* **2020**, *235*, 118262. [CrossRef]
116. Anh, N.T.; Dinh, N.X.; Van Tuan, H.; Doan, M.Q.; Khi, N.T.; Trang, V.T.; Tri, D.Q.; Le, A.-T. Eco-friendly copper nanomaterials-based dual-mode optical nanosensors for ultrasensitive trace determination of amoxicillin antibiotics residue in tap water samples. *Mater. Res. Bull.* **2021**, *147*, 111649. [CrossRef]
117. Ain, N.U.; Anis, I.; Ahmed, F.; Shah, M.R.; Parveen, S.; Faizi, S.; Ahmed, S. Colorimetric detection of amoxicillin based on querecetagetin coated silver nanoparticles. *Sens. Actuators B Chem.* **2018**, *265*, 617–624. [CrossRef]
118. Song, J.; Huang, M.; Jiang, N.; Zheng, S.; Mu, T.; Meng, L.; Liu, Y.; Liu, J.; Chen, G. Ultrasensitive detection of amoxicillin by TiO₂-g-C₃N₄@AuNPs impedimetric aptasensor: Fabrication, optimization, and mechanism. *J. Hazard. Mater.* **2020**, *391*, 122024. [CrossRef]
119. Bintsis, T. Microbial pollution and food safety. *AIMS Microbiol.* **2018**, *4*, 377–396. [CrossRef]
120. Board, O.S.; Council, N.R. Opportunities for Environmental Applications of Marine Biotechnology. Proceedings of the October 5–6, 1999, Workshop. 2000. Available online: https://books.google.com.sg/books?hl=en&lr=&id=K1ubAgAAQBAJ&oi=fnd&pg=PR1&dq=%3DBoard,+O.S.%3B+Council,+N.R.+Opportunities+for+environmental+applications+of+marine+biotechnology:+Proceedings+of+the+october+5-6,+1999,+workshop.+2000.&ots=0w23G2al-V&sig=_LvD8CDfHqVW_Oc0fZ-etBd0eZk&redir_esc=y#v=onepage&q&f=false (accessed on 30 November 2022).
121. Craun, M.F.; Craun, G.F.; Calderon, R.L.; Beach, M.J. Waterborne outbreaks reported in the United States. *J. Water Health* **2006**, *4*, 19–30. [CrossRef]
122. Pandey, P.K.; Kass, P.H.; Soupir, M.L.; Biswas, S.; Singh, V.P. Contamination of water resources by pathogenic bacteria. *AMB Express* **2014**, *4*, 51. [CrossRef]
123. Battilani, P.; Toscano, P.; Van Der Fels-Klerx, H.J.; Moretti, A.; Leggieri, M.C.; Brera, C.; Rortais, A.; Goumperis, T.; Robinson, T. Aflatoxin B1 contamination in maize in Europe increases due to climate change. *Sci. Rep.* **2016**, *6*, 24328. [CrossRef]
124. Lalah, J.O.; Omwoma, S.; Orony, D.A. Aflatoxin B1: Chemistry, Environmental and Diet Sources and Potential Exposure in Human in Kenya. In *Aflatoxin B1 Occurrence, Detection and Toxicological Effects*; Intech Open: London, UK, 2019. [CrossRef]
125. Momtaz, H.; Dehkordi, F.S.; Rahimi, E.; Asgarifar, A. Detection of Escherichia coli, Salmonella species, and Vibrio cholerae in tap water and bottled drinking water in Isfahan, Iran. *BMC Public Health* **2013**, *13*, 556–557. [CrossRef]
126. Akgönüllü, S.; Armutcu, C.; Denizli, A. Molecularly imprinted polymer film based plasmonic sensors for detection of ochratoxin A in dried fig. *Polym. Bull.* **2021**, *79*, 4049–4067. [CrossRef]
127. Sergeyeva, T.; Yarynka, D.; Lytvyn, V.; Demydov, P.; Lopatynskyi, A.; Stepanenko, Y.; Brovko, O.; Pinchuk, A.; Chegel, V. Highly-selective and sensitive plasmon-enhanced fluorescence sensor of aflatoxins. *Analyst* **2022**, *147*, 1135–1143. [CrossRef]
128. Akgönüllü, S.; Yavuz, H.; Denizli, A. SPR nanosensor based on molecularly imprinted polymer film with gold nanoparticles for sensitive detection of aflatoxin B1. *Talanta* **2020**, *219*, 121219. [CrossRef]
129. Akgönüllü, S.; Yavuz, H.; Denizli, A. Development of Gold Nanoparticles Decorated Molecularly Imprinted-Based Plasmonic Sensor for the Detection of Aflatoxin M1 in Milk Samples. *Chemosensors* **2021**, *9*, 363. [CrossRef]
130. Çimen, D.; Ashlyüce, S.; Tanalp, T.D.; Denizli, A. Molecularly imprinted nanofilms for endotoxin detection using an surface plasmon resonance sensor. *Anal. Biochem.* **2021**, *632*, 114221. [CrossRef] [PubMed]
131. Choi, S.-W.; Chang, H.-J.; Lee, N.; Kim, J.-H.; Chun, H.S. Detection of Mycoestrogen Zearalenone by a Molecularly Imprinted Polypyrrole-Based Surface Plasmon Resonance (SPR) Sensor. *J. Agric. Food Chem.* **2009**, *57*, 1113–1118. [CrossRef] [PubMed]
132. Choi, S.-W.; Chang, H.-J.; Lee, N.; Chun, H.S. A Surface Plasmon Resonance Sensor for the Detection of Deoxynivalenol Using a Molecularly Imprinted Polymer. *Sensors* **2011**, *11*, 8654–8664. [CrossRef]
133. Erdem, Ö.; Saylan, Y.; Cihangir, N.; Denizli, A. Molecularly imprinted nanoparticles based plasmonic sensors for real-time Enterococcus faecalis detection. *Biosens. Bioelectron.* **2018**, *126*, 608–614. [CrossRef] [PubMed]
134. Perçin, I.; Idil, N.; Bakhshpour, M.; Yılmaz, E.; Mattiasson, B.; Denizli, A. Microcontact Imprinted Plasmonic Nanosensors: Powerful Tools in the Detection of Salmonella paratyphi. *Sensors* **2017**, *17*, 1375. [CrossRef] [PubMed]
135. Özgür, E.; Topçu, A.A.; Yılmaz, E.; Denizli, A. Surface plasmon resonance based biomimetic sensor for urinary tract infections. *Talanta* **2020**, *212*, 120778. [CrossRef]
136. Erdem, Ö.; Cihangir, N.; Saylan, Y.; Denizli, A. Comparison of molecularly imprinted plasmonic nanosensor performances for bacteriophage detection. *New J. Chem.* **2020**, *44*, 17654–17663. [CrossRef]

137. Guo, M.; Hou, Q.; Waterhouse, G.I.; Hou, J.; Ai, S.; Li, X. A simple aptamer-based fluorescent aflatoxin B1 sensor using humic acid as quencher. *Talanta* **2019**, *205*, 120131. [[CrossRef](#)]
138. Sun, L.; Wu, L.; Zhao, Q. Aptamer based surface plasmon resonance sensor for aflatoxin B1. *Mikrochim. Acta* **2017**, *184*, 2605–2610. [[CrossRef](#)]
139. Sergeyeva, T.; Yarynka, D.; Piletska, E.; Linnik, R.; Zaporozhets, O.; Brovko, O.; Piletsky, S.; El'Skaya, A. Development of a smartphone-based biomimetic sensor for aflatoxin B1 detection using molecularly imprinted polymer membranes. *Talanta* **2019**, *201*, 204–210. [[CrossRef](#)]
140. Si, C.-Y.; Ye, Z.-Z.; Wang, Y.-X.; Gai, L.; Wang, J.-P.; Ying, Y.-B. Rapid detection of Escherichia coli O157: H7 using surface plasmon resonance (SPR) biosensor. *Spectrosc. Spectr. Anal.* **2011**, *31*, 2598–2601.
141. Yasmeen, N.; Etienne, M.; Sharma, P.S.; El-Kirat-Chatel, S.; Helú, M.B.; Kutner, W. Molecularly imprinted polymer as a synthetic receptor mimic for capacitive impedimetric selective recognition of Escherichia coli K-12. *Anal. Chim. Acta* **2021**, *1188*, 339177. [[CrossRef](#)]
142. Rehman, M.; Liu, L.; Wang, Q.; Saleem, M.H.; Bashir, S.; Ullah, S.; Peng, D. Copper environmental toxicology, recent advances, and future outlook: A review. *Environ. Sci. Pollut. Res.* **2019**, *26*, 18003–18016. [[CrossRef](#)]
143. Roney, N. *Toxicological Profile for Zinc*; Agency for Toxic Substances and Disease Registry: Atlanta, GA, USA, 2005.
144. Genchi, G.; Sinicropi, M.S.; Carocci, A.; Lauria, G.; Catalano, A. Mercury Exposure and Heart Diseases. *Int. J. Environ. Res. Public Health* **2017**, *14*, 74. [[CrossRef](#)]
145. Nordberg, M.; Nordberg, G.F. Metallothionein and Cadmium Toxicology—Historical Review and Commentary. *Biomolecules* **2022**, *12*, 360. [[CrossRef](#)]
146. Fen, Y.W.; Yunus, W.M.M. Surface plasmon resonance spectroscopy as an alternative for sensing heavy metal ions: A review. *Sens. Rev.* **2013**, *33*, 305–314. [[CrossRef](#)]
147. Safran, V.; Göktürk, I.; Derazshamshir, A.; Yılmaz, F.; Sağlam, N.; Denizli, A. Rapid sensing of Cu²⁺ in water and biological samples by sensitive molecularly imprinted based plasmonic biosensor. *Microchem. J.* **2019**, *148*, 141–150. [[CrossRef](#)]
148. Gerdan, Z.; Saylan, Y.; Uğur, M.; Denizli, A. Ion-Imprinted Polymer-on-a-Sensor for Copper Detection. *Biosensors* **2022**, *12*, 91. [[CrossRef](#)]
149. Sahu, D.; Sarkar, N.; Sahoo, G.; Mohapatra, P.; Swain, S.K. Nano silver imprinted polyvinyl alcohol nanocomposite thin films for Hg²⁺ sensor. *Sens. Actuators B Chem.* **2017**, *246*, 96–107. [[CrossRef](#)]
150. Raj, D.R.; Prasanth, S.; Vineeshkumar, T.; Sudarsanakumar, C. Surface Plasmon Resonance based fiber optic sensor for mercury detection using gold nanoparticles PVA hybrid. *Opt. Commun.* **2016**, *367*, 102–107. [[CrossRef](#)]
151. Bakhshpour, M.; Denizli, A. Highly sensitive detection of Cd(II) ions using ion-imprinted surface plasmon resonance sensors. *Microchem. J.* **2020**, *159*, 105572. [[CrossRef](#)]
152. Jalilzadeh, M.; Çimen, D.; Özgür, E.; Esen, C.; Denizli, A. Design and preparation of imprinted surface plasmon resonance (SPR) nanosensor for detection of Zn(II) ions. *J. Macromol. Sci. Part A* **2019**, *56*, 877–886. [[CrossRef](#)]
153. D'Ilio, S.; Petrucci, F.; D'Amato, M.; Di Gregorio, M.; Senofonte, O.; Violante, N. Method validation for determination of arsenic, cadmium, chromium and lead in milk by means of dynamic reaction cell inductively coupled plasma mass spectrometry. *Anal. Chim. Acta* **2008**, *624*, 59–67. [[CrossRef](#)] [[PubMed](#)]
154. Sung, Y.-M.; Wu, S.-P. Colorimetric detection of Cd(II) ions based on di-(1H-pyrrol-2-yl)methanethione functionalized gold nanoparticles. *Sens. Actuators B Chem.* **2014**, *201*, 86–91. [[CrossRef](#)]
155. Deymehkar, E.; Taher, M.A.; Karami, C.; Arman, A. Synthesis of SPR Nanosensor using Gold Nanoparticles and its Application to Copper (II) Determination. *Silicon* **2017**, *10*, 1329–1336. [[CrossRef](#)]
156. Hu, J.; Sedki, M.; Shen, Y.; Mulchandani, A.; Gao, G. Chemiresistor sensor based on ion-imprinted polymer (IIP)-functionalized rGO for Cd(II) ions in water. *Sens. Actuators B Chem.* **2021**, *346*, 130474. [[CrossRef](#)]
157. Aydoğan, N.; Aylaz, G.; Bakhshpour, M.; Tugsuz, T.; Andaç, M. Molecularly Designed Ion-Imprinted Nanoparticles for Real-Time Sensing of Cu(II) Ions Using Quartz Crystal Microbalance. *Biomimetics* **2022**, *7*, 191. [[CrossRef](#)]
158. Geens, T.; Goeyens, L.; Covaci, A. Are potential sources for human exposure to bisphenol-A overlooked? *Int. J. Hyg. Environ. Health* **2011**, *214*, 339–347. [[CrossRef](#)]
159. Fasano, E.; Esposito, F.; Scognamiglio, G.; Di Francesco, F.; Montuori, P.; Cocchieri, R.A.; Cirillo, T. Bisphenol A contamination in soft drinks as a risk for children's health in Italy. *Food Addit. Contam. Part A* **2015**, *32*, 1207–1214. [[CrossRef](#)]
160. Moriyama, K.; Tagami, T.; Akamizu, T.; Usui, T.; Saijo, M.; Kanamoto, N.; Hataya, Y.; Shimatsu, A.; Kuzuya, H.; Nakao, K. Thyroid Hormone Action Is Disrupted by Bisphenol A as an Antagonist. *J. Clin. Endocrinol. Metab.* **2002**, *87*, 5185–5190. [[CrossRef](#)]
161. Zoeller, R.T.; Bansal, R.; Parris, C. Bisphenol-A, an Environmental Contaminant that Acts as a Thyroid Hormone Receptor Antagonist in Vitro, Increases Serum Thyroxine, and Alters RC3/Neurogranin Expression in the Developing Rat Brain. *Endocrinology* **2005**, *146*, 607–612. [[CrossRef](#)]
162. Pelch, K.; Wignall, J.A.; Goldstone, A.E.; Ross, P.K.; Blain, R.B.; Shapiro, A.; Holmgren, S.D.; Hsieh, J.-H.; Svoboda, D.; Auerbach, S.S.; et al. A scoping review of the health and toxicological activity of bisphenol A (BPA) structural analogues and functional alternatives. *Toxicology* **2019**, *424*, 152235. [[CrossRef](#)]
163. Ma, Y.; Liu, H.; Wu, J.; Yuan, L.; Wang, Y.; Du, X.; Wang, R.; Marwa, P.W.; Petlulu, P.; Chen, X.; et al. The adverse health effects of bisphenol A and related toxicity mechanisms. *Environ. Res.* **2019**, *176*, 108575. [[CrossRef](#)]

164. Servos, M.; Bennie, D.; Burnison, B.; Jurkovic, A.; McInnis, R.; Neheli, T.; Schnell, A.; Seto, P.; Smyth, S.; Ternes, T. Distribution of estrogens, 17 β -estradiol and estrone, in Canadian municipal wastewater treatment plants. *Sci. Total Environ.* **2005**, *336*, 155–170. [[CrossRef](#)]
165. Malekinejad, H.; Rezaabakhsh, A. Hormones in Dairy Foods and Their Impact on Public Health—A Narrative Review Article. *Iran. J. Public Health* **2015**, *44*, 742–758.
166. Zhang, Q.; Jing, L.; Zhang, J.; Ren, Y.; Wang, Y.; Wang, Y.; Wei, T.; Liedberg, B. Surface plasmon resonance sensor for femtomolar detection of testosterone with water-compatible macroporous molecularly imprinted film. *Anal. Biochem.* **2014**, *463*, 7–14. [[CrossRef](#)]
167. Tan, Y.; Jing, L.; Ding, Y.; Wei, T. A novel double-layer molecularly imprinted polymer film based surface plasmon resonance for determination of testosterone in aqueous media. *Appl. Surf. Sci.* **2015**, *342*, 84–91. [[CrossRef](#)]
168. Çimen, D. Testosterone Imprinted poly(HEMA-MAA) Nanoparticles Based Surface Plasmon Resonance Sensor for Detection of Testosterone. *ChemistrySelect* **2022**, *7*, e202103949. [[CrossRef](#)]
169. Nawaz, T.; Ahmad, M.; Yu, J.Y.; Wang, S.Q.; Wei, T. The biomimetic detection of progesterone by novel bifunctional group monomer based molecularly imprinted polymers prepared in UV light. *New J. Chem.* **2020**, *44*, 6992–7000. [[CrossRef](#)]
170. Yu, J.Y.; Jiao, S.Q.; Nawaz, T.; Wang, S.Q.; Wei, T.X. Surface plasmon resonance sensor for biomimetic detection of progesterone with macroporous molecularly imprinted polymers prepared by visible light. *IOP Conf. Ser. Mater. Sci. Eng.* **2019**, *688*, 033032. [[CrossRef](#)]
171. Turkoglu, E.A.; Bakhshpour, M.; Denizli, A. Molecularly imprinted biomimetic surface plasmon resonance sensor for hormone detection. *Biointerface Res. Appl Chem.* **2019**, *9*, 4090–4095. [[CrossRef](#)]
172. Jiao, S.Q.; Chen, X.L.; Yu, J.Y.; Nawaz, T.; Wei, T.X. Surface plasmon resonance sensor based on Bi-monomer System (BMS) molecularly imprinted polymer for detection of 17 β -estradiol in aqueous media. *IOP Conf. Ser. Earth Environ. Sci.* **2019**, *295*, 032017. [[CrossRef](#)]
173. Torrini, F.; Palladino, P.; Baldoneschi, V.; Scarano, S.; Minunni, M. Sensitive ‘two-steps’ competitive assay for gonadotropin-releasing hormone detection via SPR biosensing and polynorepinephrine-based molecularly imprinted polymer. *Anal. Chim. Acta* **2021**, *1161*, 338481. [[CrossRef](#)] [[PubMed](#)]
174. Yockell-Lelièvre, H.; Bukar, N.; McKeating, K.S.; Arnaud, M.; Cosin, P.; Guo, Y.; Dupret-Carruel, J.; Mouglin, B.; Masson, J.-F. Plasmonic sensors for the competitive detection of testosterone. *Analyst* **2015**, *140*, 5105–5111. [[CrossRef](#)] [[PubMed](#)]
175. Liu, W.; Ma, Y.; Sun, G.; Wang, S.; Deng, J.; Wei, H. Molecularly imprinted polymers on graphene oxide surface for EIS sensing of testosterone. *Biosens. Bioelectron.* **2017**, *92*, 305–312. [[CrossRef](#)]
176. Yuan, J.; Oliver, R.; Li, J.; Lee, J.; Aguilar, M.; Wu, Y. Sensitivity enhancement of SPR assay of progesterone based on mixed self-assembled monolayers using nanogold particles. *Biosens. Bioelectron.* **2007**, *23*, 144–148. [[CrossRef](#)]
177. Luo, S.-C.; Thomas, J.L.; Guo, H.-Z.; Liao, W.-T.; Lee, M.-H.; Lin, H.-Y. Electrosynthesis of Nanostructured, Imprinted Poly(hydroxymethyl 3,4-ethylenedioxythiophene) for the Ultrasensitive Electrochemical Detection of Urinary Progesterone. *ChemistrySelect* **2017**, *2*, 7935–7939. [[CrossRef](#)]
178. Des Azevedo, S.; Lakshmi, D.; Chianella, I.; Whitcombe, M.J.; Karim, K.; Ivanova-Mitseva, P.K.; Subrahmanyam, S.; Piletsky, S.A. Molecularly Imprinted Polymer-Hybrid Electrochemical Sensor for the Detection of β -Estradiol. *Ind. Eng. Chem. Res.* **2013**, *52*, 13917–13923. [[CrossRef](#)]
179. Habauzit, D.; Armengaud, J.; Roig, B.; Chopineau, J. Determination of estrogen presence in water by SPR using estrogen receptor dimerization. *Anal. Bioanal. Chem.* **2007**, *390*, 873–883. [[CrossRef](#)]
180. Shaikh, H.; Sener, G.; Memon, N.; Bhangar, M.I.; Nizamani, S.M.; Üzek, R.; Denizli, A. Molecularly imprinted surface plasmon resonance (SPR) based sensing of bisphenol A for its selective detection in aqueous systems. *Anal. Methods* **2015**, *7*, 4661–4670. [[CrossRef](#)]
181. Zhu, C.; Zhang, L.; Chen, C.; Zhou, J. Determination of Bisphenol A using a Molecularly Imprinted Polymer Surface Plasmon Resonance Sensor. *Anal. Lett.* **2015**, *48*, 1537–1550. [[CrossRef](#)]
182. Wang, Z.; Yan, R.; Liao, S.; Miao, Y.; Zhang, B.; Wang, F.; Yang, H. In situ reduced silver nanoparticles embedded molecularly imprinted reusable sensor for selective and sensitive SERS detection of Bisphenol A. *Appl. Surf. Sci.* **2018**, *457*, 323–331. [[CrossRef](#)]
183. Uchida, A.; Kitayama, Y.; Takano, E.; Ooya, T.; Takeuchi, T. Supraparticles comprised of molecularly imprinted nanoparticles and modified gold nanoparticles as a nanosensor platform. *RSC Adv.* **2013**, *3*, 25306–25311. [[CrossRef](#)]
184. Xue, J.-Q.; Li, D.-W.; Qu, L.-L.; Long, Y.-T. Surface-imprinted core-shell Au nanoparticles for selective detection of bisphenol A based on surface-enhanced Raman scattering. *Anal. Chim. Acta* **2013**, *777*, 57–62. [[CrossRef](#)]
185. Hegnerová, K.; Piliarik, M.; Šteinbachová, M.; Flegelová, Z.; Černožorská, H.; Homola, J. Detection of bisphenol A using a novel surface plasmon resonance biosensor. *Anal. Bioanal. Chem.* **2010**, *398*, 1963–1966. [[CrossRef](#)]
186. Anirudhan, T.S.; Athira, V.S.; Sekhar, V.C. Electrochemical sensing and nano molar level detection of Bisphenol-A with molecularly imprinted polymer tailored on multiwalled carbon nanotubes. *Polymer* **2018**, *146*, 312–320. [[CrossRef](#)]
187. Patel, A.B.; Shaikh, S.; Jain, K.R.; Desai, C.; Madamwar, D. Polycyclic Aromatic Hydrocarbons: Sources, Toxicity, and Remediation Approaches. *Front. Microbiol.* **2020**, *11*, 562813. [[CrossRef](#)]
188. Adeniji, A.O.; Okoh, O.O.; Okoh, A.I. Levels of Polycyclic Aromatic Hydrocarbons in the Water and Sediment of Buffalo River Estuary, South Africa and Their Health Risk Assessment. *Arch. Environ. Contam. Toxicol.* **2019**, *76*, 657–669. [[CrossRef](#)]

189. Srogi, K. Monitoring of environmental exposure to polycyclic aromatic hydrocarbons: A review. *Environ. Chem. Lett.* **2007**, *5*, 169–195. [[CrossRef](#)]
190. Ravindra, K.; Sokhi, R.; Van Grieken, R. Atmospheric polycyclic aromatic hydrocarbons: Source attribution, emission factors and regulation. *Atmos. Environ.* **2008**, *42*, 2895–2921. [[CrossRef](#)]
191. Abdel-Shafy, H.I.; Mansour, M.S.M. A review on polycyclic aromatic hydrocarbons: Source, environmental impact, effect on human health and remediation. *Egypt. J. Pet.* **2016**, *25*, 107–123. [[CrossRef](#)]
192. Gupte, A.; Tripathi, A.; Patel, H.; Rudakiya, D.; Gupte, S. Bioremediation of Polycyclic Aromatic Hydrocarbon (PAHs): A Perspective. *Open Biotechnol. J.* **2016**, *10*, 363–378. [[CrossRef](#)]
193. Mojiri, A.; Zhou, J.L.; Ohashi, A.; Ozaki, N.; Kindaichi, T. Comprehensive review of polycyclic aromatic hydrocarbons in water sources, their effects and treatments. *Sci. Total Environ.* **2019**, *696*, 133971. [[CrossRef](#)] [[PubMed](#)]
194. Rengarajan, T.; Rajendran, P.; Nandakumar, N.; Lokeshkumar, B.; Rajendran, P.; Nishigaki, I. Exposure to polycyclic aromatic hydrocarbons with special focus on cancer. *Asian Pac. J. Trop. Biomed.* **2015**, *5*, 182–189. [[CrossRef](#)]
195. Burchiel, S.W.; Gao, J. Polycyclic Aromatic Hydrocarbons and the Immune System. In *Encyclopedia of Immunotoxicology*; Vohr, H.-W., Ed.; Springer: Berlin/Heidelberg, Germany, 2005; pp. 1–7.
196. Bolden, A.L.; Rochester, J.R.; Schultz, K.; Kwiatkowski, C.F. Polycyclic aromatic hydrocarbons and female reproductive health: A scoping review. *Reprod. Toxicol.* **2017**, *73*, 61–74. [[CrossRef](#)]
197. Yan, J.; Wang, L.; Fu, P.P.; Yu, H. Photomutagenicity of 16 polycyclic aromatic hydrocarbons from the US EPA priority pollutant list. *Mutat. Res. Genet. Toxicol. Environ. Mutagen.* **2004**, *557*, 99–108. [[CrossRef](#)]
198. Yu, H. Environmental carcinogenic polycyclic aromatic hydrocarbons: Photochemistry and phototoxicity. *J. Environ. Sci. Health Part C* **2002**, *20*, 149–183. [[CrossRef](#)]
199. Ghosal, D.; Ghosh, S.; Dutta, T.K.; Ahn, Y. Current state of knowledge in microbial degradation of polycyclic aromatic hydrocarbons (PAHs): A review. *Front. Microbiol.* **2016**, 1369. [[CrossRef](#)]
200. Rajpara, R.K.; Dudhagara, D.R.; Bhatt, J.K.; Gosai, H.B.; Dave, B.P. Polycyclic aromatic hydrocarbons (PAHs) at the Gulf of Kutch, Gujarat, India: Occurrence, source apportionment, and toxicity of PAHs as an emerging issue. *Mar. Pollut. Bull.* **2017**, *119*, 231–238. [[CrossRef](#)]
201. Perera, F.P.; Chang, H.W.; Tang, D.; Roen, E.L.; Herbstman, J.; Margolis, A.; Huang, T.J.; Miller, R.L.; Wang, S.; Rauh, V. Early-life exposure to polycyclic aromatic hydrocarbons and ADHD behavior problems. *PLoS ONE* **2014**, *9*, e111670. [[CrossRef](#)]
202. Burchiel, S.W.; Luster, M.I. Signaling by Environmental Polycyclic Aromatic Hydrocarbons in Human Lymphocytes. *Clin. Immunol.* **2001**, *98*, 2–10. [[CrossRef](#)]
203. Hrudková, M.; Fiala, Z.; Borská, L.; Novosad, J.; Smolej, L. The effect of polycyclic aromatic hydrocarbons to bone marrow. *Acta Med. Suppl.* **2004**, *47*, 75–81.
204. Nowakowski, M.; Rykowska, I.; Wolski, R.; Andrzejewski, P. Polycyclic Aromatic Hydrocarbons (PAHs) and their Derivatives (O-PAHs, N-PAHs, OH-PAHs): Determination in Suspended Particulate Matter (SPM)—A Review. *Environ. Process.* **2021**, *9*, 2. [[CrossRef](#)]
205. Yang, M.; Tian, S.; Liu, Q.; Yang, Z.; Yang, Y.; Shao, P.; Liu, Y. Determination of 31 Polycyclic Aromatic Hydrocarbons in Plant Leaves Using Internal Standard Method with Ultrasonic Extraction–Gas Chromatography–Mass Spectrometry. *Toxics* **2022**, *10*, 634. [[CrossRef](#)]
206. Nsibande, S.; Montaseri, H.; Forbes, P. Advances in the application of nanomaterial-based sensors for detection of polycyclic aromatic hydrocarbons in aquatic systems. *TrAC Trends Anal. Chem.* **2019**, *115*, 52–69. [[CrossRef](#)]
207. Wang, D.; Hui, B.; Zhang, X.; Zhu, J.; Gong, Z.; Fan, M. Facile Preparation of Ag-NP-Deposited HRGB-SERS Substrate for Detection of Polycyclic Aromatic Hydrocarbons in Water. *Chemosensors* **2022**, *10*, 406. [[CrossRef](#)]
208. Castro-Grijalba, A.; Montes-García, V.; Cordero-Ferradás, M.J.; Coronado, E.A.; Pérez-Juste, J.; Pastoriza-Santos, I. SERS-Based Molecularly Imprinted Plasmonic Sensor for Highly Sensitive PAH Detection. *ACS Sensors* **2020**, *5*, 693–702. [[CrossRef](#)]
209. Yu, Z.; Grasso, M.F.; Sorensen, H.H.; Zhang, P. Ratiometric SERS detection of polycyclic aromatic hydrocarbons assisted by β -cyclodextrin-modified gold nanoparticles. *Microchim. Acta* **2019**, *186*, 391. [[CrossRef](#)]
210. Huang, J.; Zhou, T.; Zhao, W.; Cui, S.; Guo, R.; Li, D.; Reddy Kadasala, N.; Han, D.; Jiang, Y.; Liu, Y.; et al. Multifunctional magnetic Fe₃O₄/Cu₂O-Ag nanocomposites with high sensitivity for SERS detection and efficient visible light-driven photocatalytic degradation of polycyclic aromatic hydrocarbons (PAHs). *J. Colloid Interface Sci.* **2022**, *628*, 315–326. [[CrossRef](#)]
211. Capaccio, A.; Sasso, A.; Rusciano, G. Feasibility of SERS-Active Porous Ag Substrates for the Effective Detection of Pyrene in Water. *Sensors* **2022**, *22*, 2764. [[CrossRef](#)]
212. Lellis, B.; Fávoro-Polonio, C.Z.; Pamphile, J.A.; Polonio, J.C. Effects of textile dyes on health and the environment and bioremediation potential of living organisms. *Biotechnol. Res. Innov.* **2019**, *3*, 275–290. [[CrossRef](#)]
213. Lara, L.; Cabral, I.; Cunha, J. Ecological Approaches to Textile Dyeing: A Review. *Sustainability* **2022**, *14*, 8353. [[CrossRef](#)]
214. Mahapatra, N. *Textile Dyes*; CRC Press: Boca Raton, FL, USA, 2016.
215. Khan, S.; Malik, A. Toxicity evaluation of textile effluents and role of native soil bacterium in biodegradation of a textile dye. *Environ. Sci. Pollut. Res.* **2017**, *25*, 4446–4458. [[CrossRef](#)] [[PubMed](#)]
216. Copaciu, F.; Opreș, O.; Coman, V.; Ristoiu, D.; Niinemets, Ü.; Copolovici, L. Diffuse Water Pollution by Anthraquinone and Azo Dyes in Environment Importantly Alters Foliage Volatiles, Carotenoids and Physiology in Wheat (*Triticum aestivum*). *Water Air Soil Pollut.* **2013**, *224*, 1478. [[CrossRef](#)]

217. Clark, M. *Handbook of Textile and Industrial Dyeing: Principles, Processes and Types of Dyes*; Elsevier: Amsterdam, The Netherlands, 2011.
218. Christie, R.M. *Environmental Aspects of Textile Dyeing*; Elsevier: Amsterdam, The Netherlands, 2007. [[CrossRef](#)]
219. Thakur, I.S. *Environmental Biotechnology: Basic Concepts and Applications*; IK International: Delhi, India, 2006.
220. Hunger, K. *Industrial Dyes: Chemistry, Properties, Applications*; John Wiley & Sons: Hoboken, NJ, USA, 2007.
221. Lacasse, K.; Baumann, W. *Textile Chemicals: Environmental Data and Facts*; Springer Science & Business Media: Berlin/Heidelberg, Germany, 2012.
222. Liu, X.; Qi, X.; Zhang, L. 3D hierarchical magnetic hollow sphere-like CuFe₂O₄ combined with HPLC for the simultaneous determination of Sudan I–IV dyes in preserved bean curd. *Food Chem.* **2017**, *241*, 268–274. [[CrossRef](#)] [[PubMed](#)]
223. Schummer, C.; Sassel, J.; Bonenberger, P.; Moris, G. Low-Level Detections of Sudan I, II, III and IV in Spices and Chili-Containing Foodstuffs Using UPLC-ESI-MS/MS. *J. Agric. Food Chem.* **2013**, *61*, 2284–2289. [[CrossRef](#)]
224. Dil, E.A.; Ghaedi, M.; Asfaram, A. Optimization and modeling of preconcentration and determination of dyes based on ultrasound assisted-dispersive liquid–liquid microextraction coupled with derivative spectrophotometry. *Ultrason. Sonochem.* **2017**, *34*, 27–36. [[CrossRef](#)]
225. Xue, Y.; Shao, J.; Sui, G.; Ma, Y.; Li, H. Rapid detection of orange II dyes in water with SERS imprinted sensor based on PDA-modified MOFs@Ag. *J. Environ. Chem. Eng.* **2021**, *9*, 106317. [[CrossRef](#)]
226. Li, H.; Li, D.; Wang, J.; Yu, H.; Huang, C.; Jiang, W.; Liu, C.; Che, G.; Wang, D. A novel imprinted sensor based on Ag-modified composite MOFs for selective detection of Rhodamine B in river. *J. Environ. Chem. Eng.* **2022**, *10*, 108163. [[CrossRef](#)]
227. Li, H.; Jiang, J.; Wang, Z.; Wang, X.; Liu, X.; Yan, Y.; Li, C. A high performance and highly-controllable core-shell imprinted sensor based on the surface-enhanced Raman scattering for detection of R6G in water. *J. Colloid Interface Sci.* **2017**, *501*, 86–93. [[CrossRef](#)]
228. Li, H.; Wang, X.; Wang, Z.; Jiang, J.; Wei, M.; Zheng, J.; Yan, Y.; Li, C. Thermo-responsive molecularly imprinted sensor based on the surface-enhanced Raman scattering for selective detection of R6G in the water. *Dalton Trans.* **2017**, *46*, 11282–11290. [[CrossRef](#)]
229. Xu, X.-Y.; Tian, X.-G.; Cai, L.-G.; Xu, Z.-L.; Lei, H.-T.; Wang, H.; Sun, Y.-M. Molecularly imprinted polymer based surface plasmon resonance sensors for detection of Sudan dyes. *Anal. Methods* **2014**, *6*, 3751–3757. [[CrossRef](#)]
230. Ding, G.; Xie, S.; Liu, Y.; Wang, L.; Xu, F. Graphene oxide-silver nanocomposite as SERS substrate for dye detection: Effects of silver loading amount and composite dosage. *Appl. Surf. Sci.* **2015**, *345*, 310–318. [[CrossRef](#)]
231. Adade, S.Y.-S.S.; Lin, H.; Haruna, S.A.; Barimah, A.O.; Jiang, H.; Agyekum, A.A.; Johnson, N.A.N.; Zhu, A.; Ekumah, J.-N.; Li, H.; et al. SERS-based sensor coupled with multivariate models for rapid detection of palm oil adulteration with Sudan II and IV dyes. *J. Food Compos. Anal.* **2022**, *114*, 104834. [[CrossRef](#)]

Disclaimer/Publisher’s Note: The statements, opinions and data contained in all publications are solely those of the individual author(s) and contributor(s) and not of MDPI and/or the editor(s). MDPI and/or the editor(s) disclaim responsibility for any injury to people or property resulting from any ideas, methods, instructions or products referred to in the content.